FRICTION STIR WELDING (FSW) OF DISSIMILAR METALS AND ALLOYS

BY

GIHAD MOHAMED KARRAR BABEKR

A Thesis Presented to the
DEANSHIP OF GRADUATE STUDIES

KING FAHD UNIVERSITY OF PETROLEUM & MINERALS

DHAHRAN, SAUDI ARABIA

In Partial Fulfillment of the
Requirements for the Degree of

MASTER OF SCIENCE

In

MECHANICAL ENGINEERING

JANUARY, 2015

KING FAHD UNIVERSITY OF PETROLEUM & MINERALS

DHAHRAN- 31261, SAUDI ARABIA

DEANSHIP OF GRADUATE STUDIES

This thesis, written by **Gihad Mohamed Karrar** under the direction of his thesis advisor and approved by his thesis committee, has been presented and accepted by the Dean of Graduate Studies, in partial fulfillment of the requirements for the degree of **MASTER OF SCIENCE IN MECHANICAL ENGINEERING.**

Dr. Abdelrahman Nasr Shuaib
(Advisor)

Dr. Neçar Merah
(Member)

Dr. Abdelaziz Bazoune
(Member)

Dr. Zuhair M. Gasem
Department Chairman

Dr. Salam A. Zummo
Dean of Graduate Studies

22/1/15

Date

January 2015

Dedication

To My Parents, My Wife and My Colleagues with love.

ACKNOWLEDGEMENTS

All praise is due to almighty ALLAH, the most compassionate the most merciful who gave me the strength, knowledge and patience to complete this work.

I would like to acknowledge KFUPM for granting me this opportunity to pursue my graduate studies and providing all kinds of support.

I would also like to acknowledge the support provided by King Abdulaziz City for Science and Technology (KACST) through the Science and Technology Unit at King Fahd University of Petroleum and Minerals (KFUPM) for funding this work through Project No. 11-ADV2130-04.

I would like to express my gratitude to my supervisor, Dr. Abdelrahman Nasr Shuaib for his guidance, understanding, patience, and most importantly, his friendship during my graduate studies at KFUPM. I would also like to thank members of my committee, Dr. Neçar Merah, and Dr. Abdelaziz Bazoune for the assistance they provided at all levels of the research project.

Grateful thanks to the man who helped me a lot during this research, Dr. Fadi Abdel Kareem Al-Badour.

Thanks a lot to my research group, Dr. Zafr Iqbal and Mr. Ahmed Kamal.

A special thanks is due to my family for their enormous love, support and prayers.

TABLE OF CONTENTS

LIST OF TABLES

LIST OF FIGURES

ABSTRACT (ENGLISH)

Full Name : Gihad Mohamed Karrar Babekr

Thesis Title : FRICTION STIR WELDING (FSW) OF DISSIMILAR METALS AND ALLOYS

Major Field : Mechanical Engineering

Date of Degree : January 2015

The mismatch in physical and mechanical properties between two dissimilar materials, such as aluminum and copper, presents significant technological challenges when fusion welding processes are used to join them. This is the reason for considering friction stir welding for these applications. This work presents the results of performing successful butt welding of aluminum grade Al6061-T6 to commercial pure copper using the relatively new friction stir welding (FSW) process. The main objective of the present work is to develop a process based on friction stir welding (FSW) to weld similar and dissimilar materials of aluminum grade Al6061-T6 and commercial pure copper. Finite element models will be also used to simulate the joining process and study the effects of the process parameters on the weld features. After analyzing the results, it has been found that the process parameters of similar FSW butt joints are totally different from those of dissimilar FSW parameters, where it is difficult to achieve a defect free joint for dissimilar materials by considering the traditional method. Dissimilar aluminum to copper FSW defect free joint was obtained under the condition of offsetting the tool 2 mm toward the retreating side and locating the harder material (Cu) on the advancing side at 40 mm/min welding speed and 900 rpm rotational speed.

ABSTRACT (ARABIC)

ملخص الرسالة

الاسم الكامل : جهاد محمد كرار بابكر

عنوان الرسالة : اللحام التحريكي الاحتكاكي للمعادن والسبائك المختلفة

التخصص : الهندسة الميكانيكية

تاريخ الدرجة العلمية : ربيع الاول ١٤٣٦ هـ

ان تباين الخواص الفيزيائية والكيميائية بين مادتين مختلفتين كالنحاس والالمونيوم ابرز تحديا تقنيا حقيقيا عند استخدام اللحام التقليدي للحم هاتين المادتين, لهذا تم اعتبار طريقة اللحام التحريكي الاحتكاكي كوسيلة ناجحه لمثل هذه التطبيقات. في هذا البحث يتم عرض نتائج ناجحه للحم كل من الالمونيوم للالمونيوم, النحاس للنحاس والامونيوم للنحاس باستخدام تقنية حديثة نسبيا وهي اللحام التحريكي الاحتكاكي. ان الهدف الرئيسي لهذا البحث هو تطوير عملية اللحام التحريكي الاحتكاكي للحم مواد متشابه ومختلفه من الالمونيوم والنحاس. بالاضافة الى ذلك تم اعتبار الطرق العددية للتحليل لمحاكاة عملية اللحام ودراسة تأثير المتغيرات على الوصلات المتكونه. بعد تحليل النتائج ودراستها وجد ان عوامل اللحام للمواد المتشابه تختلف تماما عنها للمواد المختلفة حيث انه من الصعب الحصول على وصلة جيده لمادتين مختلفتين بالطرق العملية التقليدية خاصة اذا كان الاختلاف في الخواص الميكانيكية والحرارية كبيرا. وقد تم التوصل الى وصلة خالية من الفراغات لمادتي الالمونيوم والنحاس باعتبار طريقة ازاحة اداة اللحام مسافة ٢ مم الى جهة الماده الاضعف ووضع الماده الاقوى (النحاس) ناحية الجانب التقدمي للوصلة وبسرعة لحام ٤٠ مم\ث وسرعة دوران بلغت ٩٠٠ لفة في الدقيقة.

CHAPTER 1

INTRODUCTION

1.1 Background

No doubt friction stir welding (FSW) technology can be considered as one of the most significant processes that have been developed in solid-phase joining techniques for the last two decades. This welding technique appeared in 1991 and has been patented by Technical Welding Institute (TWI) in 1994 [1]. This process has several potential applications in the domains of automotive, aerospace and shipbuilding industries in addition to the military fields.

Friction stir welding is a simple process that consists of several steps including:

- The rotation of a specific design tool-named as the friction stir tool- without any action on the workpiece.
- The plunging step, where the pin tool penetrates the workpiece, while it is rotating. This leads to heating the material to a temperature close to its melting point resulting in plasticizing it. This step ends when the tool shoulder contacts the upper surface of the workpiece at the location where the welding starts.
- At contact between the pin tool shoulder and the workpiece surface, the rotating friction stir tool starts its traversing motion along the welding direction or the process zone path. During this phase heat is generated due to friction between the tool and the workpiece. Both pin-shoulder geometry and tool rotation action cause

the plasticized material to move from the advancing side to the retreating side. During this phase of the welding process, the pin shoulder mission is to encapsulate the material below it.

- Upon reaching the end of the welding path, the tool is retracted from the joint leaving a hole that indicates the last pin location.

Normally, during friction stir welding, the work pieces are clamped on backing plate where vertical, lateral as well as longitudinal movements have to be prevented. The process can be considered as forging –extrusion process as shown in Figure 1, which also includes the process terminologies.

FSW as a joining process has many advantages against the conventional fusion welding, including [2], use of non-consumable tool, no filler wire, no gas shielding for Al-alloys, no welder or process qualification, some tolerance of imperfect weld preparation (thin oxide layers can be accepted), low distortion even in long welds, excellent mechanical properties, no fume, porosity and spatter as well as operable in many positions.

In contrast, the drawbacks of this technique include:

- Special attention should be given the work piece clamping.

- Because there is no filler material normally the workpiece thickness may be reduced, unless an allowance is provided during joint design.

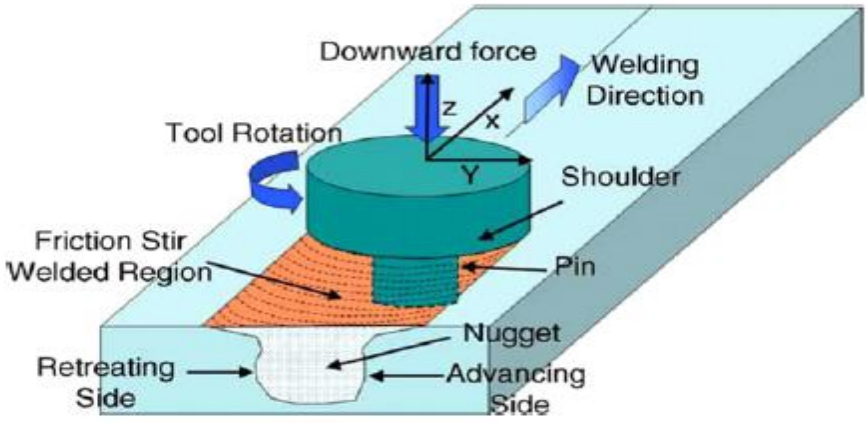

Fig. 1.1: Schematic Illustration of FSW Process [1]

1.2 Dissimilar Metals and Alloys Joining Processes

The wide variety in physical and mechanical properties among various classes of metals and alloys enable users to select various combinations of these materials to meet desired service conditions. There are many examples for use of dissimilar metal/alloy combinations for engineering components and equipment. For instance, power systems use combinations of austenitic/ferritic steels and oil and gas industry uses cupronickel/ steel. Copper alloys/steel are used for marine engineering applications and aluminum alloys/steel and titanium are used in transportation and aerospace industry.

Depending on the joint requirements and materials combinations, several joining process can be used for joining dissimilar materials such as: Fusion Welding, Diffusion Bonding, Brazing, Glazing, Adhesive Bonding as well as Mechanical Attachment. The success of dissimilar materials joining depends on using the appropriate process and corresponding

parameters. Fusion welding is the most popular conventional joining process for dissimilar metals in spite of its numerous shortcomings [3].

The challenges experienced when welding a pair of dissimilar metals/alloys using conventional fusion welding processes arise from the mismatch in their physical and mechanical properties. For example the difference in melting point temperature impairs the fusion process. The difference in thermal expansion leads to a large formation of residual stresses that reduce the joining process strength. Likewise the thermal conductivity difference complicates the joining process too.

As mentioned above, there is an increasing trend in the use of parts made form dissimilar materials. For example dissimilar materials are being used in aircrafts and cars to decrease energy consumption. Nowadays, joining of dissimilar materials is favorable since it provides designers the ability to enhance the performance of their products by combining different materials to meet the functional requirements of a part. However, this important use poses a number of fabrication challenges, including welding.

Several techniques have been developed for joining aluminum to steel or to other aluminum alloys. These methods include, adhesive bonding, riveting, spot welding, fusion welding, clinching and laser roll welding. These techniques show many problems like, excessive heating, poor structural stability, poor seam surface of the weld and defects formation which hinder the application of these methods [3]. On the other hand, the relatively new friction stir welding (FSW) as a solid state welding process has shown

promising results for joining dissimilar metals with free defects and high strength joints compared to fusion welding.

Conventional fusion welding process requires significant amounts of heat input that leads to change the microstructure and the mechanical properties of the dissimilar materials joint. On the other hand, friction stir welding that has low heat input and subjects the joint to plastic deformation can produce efficient dissimilar joints compared to fusion welding [4].

1.3 Problem Statement and Objectives

The mismatch in physical and mechanical properties between two dissimilar materials, such as aluminum and copper, presents significant technological challenges when fusion welding processes are used to join them. This is the reason for considering friction stir welding for these applications. This work presents the results of performing successful butt welding of aluminum grade Al6061-T6 to commercial pure copper using the relatively new friction stir welding (FSW) process.

The main objective of the present work is to develop a process based on -friction stir welding (FSW)- to weld similar and dissimilar materials of aluminum grade Al6061-T6 and commercial pure copper. The specific objectives include:

- Finding friction stir welding process parameters that will produce sound (FSW) butt joints of copper to copper, aluminum to aluminum and dissimilar copper to aluminum.

- Evaluating the effects of the friction stir weld parameter on the quality of the weldment using metallurgical analytical and mechanical techniques.
- Developing a finite element model to simulate the friction stir welding process and understand the effects of the process parameters on the process dependent variables such as temperature, developed stresses, and strains.

1.4 Research Approach

The objectives of this investigation will be achieved using experimental and numerical modeling techniques. Butt welds will be performed using a fully instrumented FSW machine developed by Shuaib et al [5] on copper-to-copper, aluminum-to-aluminum and copper-to-aluminum plates. The quality of the weldment is evaluated using metallurgical, mechanical testing, and SEM/EDS techniques. The finite element models will be also used to simulate the joining process and study the effects of the process parameters on the weld features. The experimental results and the finite element results together with the phase diagrams of metals and alloys are used to determine the phases and composition of the nugget.

1.5 Thesis Layout

This thesis includes six chapters: Chapter one is an introduction to the present work and its objectives. Chapter two is a literature review that covers the issues related to the criteria behind friction stir welding process as well as friction stir welding of similar and dissimilar materials. Chapter three covers the experimental setups and work for achieving FSW butt joints of similar and dissimilar aluminum and copper. Chapter four includes the

several finite element models which are developed or modified in order to simulate the friction stir welding process. Chapter five explains the results analysis and discussion of both similar and dissimilar friction stir butt welding joints. Finally, Chapter six includes the research conclusion and recommendations for future works.

CHAPTER 2

Literature Review

This chapter covers technical literature review of the issues associated with the friction stir welding process as well as the welding of dissimilar metals and alloys using FSW. This includes tool material and design, types of base metals and alloys, effects of process parameters on weld quality, and finite element modeling of FSW process.

2.1 FSW Tool Design and Materials

Friction stir welding tool consists of two main parts, the tool shoulder and the tool pin. The tool shoulder role is to generate the friction heat -between the workpiece and the pin too- as well as apply the forging load which is necessary for joint consolidation, whereas the pin stirs the softened joint materials and facilitates mixing them. The two important factors that influence shoulder design are joint shape and the thickness of the welded parts.

Scialpi et.al [6], studied the effect of different shoulder geometries (scroll with fillet, cavity with fillet and only fillet) on the mechanical properties on 6082-T6 aluminum alloy. The sample thickness was 1.5 mm while the welding process was carried out at 1810 rpm with feed rate of 460 mm/min. They observed that the tool with cavity and fillet shoulder showed the best crown and root quality off the butt joints. Transverse and tensile strength of the three designs registered non-considerable difference where the longitudinal tensile tests showed large differences. This could be attributed to the higher strength and elongation of the tool with [fillet+ scroll and tool with fillet and shoulder]

compared to tool with fillet shoulder only. They concluded that tool with fillet and cavity could be the best because it increases the longitudinal and transverse strength as well as provides the best crown surface.

In another interesting effort, Malarvizhi and Balasubramanian [7], studied the influence of the tool shoulder diameter to plate thickness ratio (D/T) on stir zone formation and tensile properties for dissimilar joint-AA6061 aluminum and AZ31B magnesium alloys. They found that tensile properties of 21 mm shoulder diameter i.e. 3.5 times the plate thickness yielded a maximum tensile strength of 192 MPa and joint efficiency of 89% compared to the lower strength base metal. In contrast, tool pin profile is another important factor on FSW process since it effects on the material flow, welding force and defects formation of FSW weld joints.

Elangovan et al [8], investigated the influences of tool pin profile and tool shoulder diameter on the formation of friction stir processing zone in AA6061 aluminum alloy, Five pin profiles (straight cylindrical, tapered cylindrical, threaded cylindrical, triangle and square) have been examined with three different shoulders. By characterizing the macro structure of the joints to observe the friction stir process zone (FSP) zone shape, height and width at three different locations, they found that the formation of the defect free friction stir process zone is a function of tool pin profile and tool shoulder diameter.

Olvier et al [9], tried to understand the material flow path during FSW process by using unthreaded tools. They used two different pin profiles (cylindrical and tapered cylindrical pin) having concave shoulder. The tool was tilted by 2.5° to provide extra compression

force to the welded stir zone. They noticed that unthreaded pins have a material flow features similar to the treaded ones. The joint zone in the cylinder pin was found to be more affected by the plunge force and rotational speed than the tapered cylindrical pin.

2.2 The effect of Process parameters and Optimization Methods

In this section, the effect of welding parameters i.e. tool rotational speed and welding speed on microstructure and mechanical properties of joints will be considered. These parameters have a large influence on the heat input per unit length of welding, which governs the joints properties and strength. On the other hand, the optimization efforts of these parameters for obtaining high efficiency welded joints will be presented.

FSW process parameters can be divided into: dependent and independent parameters. The independent parameters are the tool rotational speed and the traverse speed, while the dependent parameters are: the axial load (forging load), torque and temperature. The effects of these parameters have been studied and summarized by Mishra et.al [10].

Numerous research works has been reported. Chaitayna et al [11], tried to find the relationship among the FSW parameters on the microstructure and mechanical properties of the welded joint strictly on AA7039 aluminum alloys. They varied welding and rotary speed of the tool in order to study their effects. Their investigation showed that the mechanical properties increase by decreasing the welding speed and increasing the tool rotation speed. They also noticed that increasing the tool rotation speed and decreasing the welding speed reduces the zigzag line formation tendency. Moreover, they found that the minimum hardness region shifts from the heat affected zone (HAZ) to the weld

nugget zone (WNZ) as a result of increasing the welding speed and decreasing the tool rotation speed.

The material location with respect to the advanced and retreating sides of the advancing tool has an influence on the microstructure and tensile strength of dissimilar stir welded joints. Specifically aluminum alloys have been considered in several research papers. Dinaharan et al [12], studied the effect of tool rotational speed on the mechanical properties of dissimilar joints of aluminum alloys. They made eight joints at four different rotational speeds while changing the location of the cast and wrought AA6061 aluminum alloys between the advancing and retreating sides. They concluded that the relative material location changes the pattern of the flow during the welding process. According to this investigation, maximum tensile strength value of dissimilar materials joints was obtained when cast aluminum alloy occupied the advancing side of the tool.

The optimization of the FSW process parameters represent a great challenge nowadays especially for dissimilar joints. Koilraj et al [13], attempted to find the optimum parameters by using Taguchi L16 orthogonal design technique of experiments. They used rotational speed, traverse speed, tool geometry and ratio between shoulder to pin diameter as the main independent parameters and the joint tensile strength as the response. The cylindrical pin profiles were found to be the best among the other tool profiles. They also noticed that D/d ratio has the largest share on the tensile strength of the joints, among the other parameters.

Maximizing fatigue life and minimizing defects formation during friction stir welding process can also be considered as an effort of process parameters optimization. In an attempt to optimize the FSW process for joining 5083-H321 aluminum alloy, Lombard et al [14] considered the effects of tool rotational speed together with the welding speed on frictional input power. They found that rotational speed affects the defect occurrences. They also found that there is a strong correlation between frictional power input, tensile strength and low cycle fatigue life. These findings could be attributed to the role of the defects in inducing cracks that grow by low cycle fatigue.

2.3 FSW of Similar and Dissimilar Aluminum Alloys

One of the most attractive features of friction stir welding is the capability to join what is being classified as un welded materials by conventional fusion welding processes. FSW has been used to weld both similar and dissimilar aluminum alloys such as 2xxx, 5xxx, 6xxx and 7xxx series. Several applications have been considered in FSW. Many investigations of FSW of aluminum series materials have been conducted to study the optimum parameters for obtaining acceptable joints quality and high strength during the process. Murr [15], summarized these research efforts which span over a period of a decade and half. These studies involved FSW of 18 joint systems made of same materials and 25 joints of different dissimilar material systems. This review of FSW of similar and dissimilar aluminum series included compiling optimum experimental welding parameters (pin rotation and traverse speed). Based on his work FSW parameters for similar and dissimilar systems of aluminum alloys are now available for achieving sound weld butt joints

2.4 FSW of Similar Pure Copper

Copper and its alloys have a wide range of engineering applications. The attractive properties of copper such as high electrical and thermal conductivities as well as excellent resistance to corrosion is expanding its use as a structural material, which undergoes various manufacturing processes including joining by welding. Weldability of copper and its alloys using conventional arc welding processes is affected by a number of factors. These include, the alloying elements, the thermal conductivity of the alloy being welded, the shielding gas, the type of current used during welding, the joint design, the welding position, and the surface condition and cleanliness. For example, when welding commercial coppers and lightly alloyed copper materials with high thermal conductivities, the type of current and shielding gas must be selected to provide maximum heat input to the joint to counteract the rapid heat dissipation away from the localized weld zone. Furthermore, depending on section thickness, preheating may be required for copper alloys with lower thermal conductivities. Welded copper alloys may develop residual stresses and hot shortness.

To overcome these challenges many researches have conducted both experimental and numerical studies to use FSW in joining copper. Sakthivel and Muhopadhyay [16], applied friction stir welding technique to join 2 mm sheet thickness of commercial copper at low welding speed of 30mm/min and high rotational speed of 1000 rpm. A sound weld joint was obtained; they evaluated the welded joints by conducting both mechanical and microstructural analysis where 85% joint efficiency was recorded. Welding parameters effects on microstructure and mechanical properties were investigated by Sun and Fujii

[17] in order to specify process window for commercial pure copper in terms of welding speed, spindle speed and tool load. They recommended that increasing the applied load improves the joint mechanical strength compare to decreasing the tool rotational speed.

Established work to study the welding speed at constant rotational speed of pure copper butt joint was presented by Shen et.al [18], they proved that ultimate tensile strength as well as nugget zone grains size increasing firstly then decreasing by increasing the welding speed. They reported that at a range of 25-150 mm/min tool traverse speed has a little effect on the joint mechanical strength.

Modeling of FSW for pure copper joints is a relatively new area of research since there are only few basic works, Zadeh et.al [19] tried to develop a mathematical model that predict the tensile strength of copper joints. Response surface methodology has been considered with four different parameters: spindle speed, traveling speed, forging force and tool design. Five levels and 31 run with the help of design expert software. They observed that increasing of tool rotational speed , forging force and traveling speed increases the joints mechanical strength where the optimum condition was at 942 rpm rotational speed, 84mm/min feed rate and 1.62 KN axial force.

Another work in this direction was presented by Pashazadeh and Teimournezhad [20]. They developed an arbitrary Lagrangian Eulerian (ALE) model of FSW for copper sheet using Deform-3D capability. Their model outputs were (temperature distributions, effective plastic strain, as well as material flow). They pointed that most of the material flow close to the top surface causing a non-symmetrical shape of stir zone. They also

noticed that near to advancing side (AS) plastic strain is higher than retreating side (RS) but away from the pin zone retreating side results were greater as a result TMAZ on RS is larger than AS.

By neglecting the plastic deformation and applying moving coordinate system technique, Jabbari [21] developed a thermal model of 4 mm thickness for commercial copper plate at constant traveling speed of 25 mm/min and five different rotational speeds. The model temperature results were used to simulate the grain growth trend for copper plates. His observations were that nugget zone grain size increases by increasing tool rotational speed and at speed of 900 rpm joint maximum tensile strength as well as maximum Vickers's hardness.

2.5 FSW of Dissimilar Aluminum alloys and Copper

It is possible to partially or completely replace copper with aluminum for several engineering applications because aluminum shares with copper some similar physical properties, e.g. electrical conductivity and because aluminum has lower price and lower density. Therefore, researchers are striving to join these two metals together, while facing many challenges, including differences in chemical compositions and physical and mechanical properties. Based on its relative advantages against conventional fusion welding processes, researchers investigated the possibility of using FSW technique to replace the conventional joining methods in joining dissimilar metals and alloys and achieve better quality weld joints. For example, Li et al [22] investigated the microstructure and mechanical properties of aluminum alloys-1350 and copper butt join using FSW technique. They concluded that, both AL-1350 and Cu microstructures are

refined at the end of welding with an absence of any intermetallic compound. They also found that, at the nugget region copper hardness was greater than that of Al-1350. Galvão et al [23], studied the effect of aluminum alloy type on lap joints of aluminum and copper.

In the pioneering work Ouyang et al [24], the authors studied the microstructural evolution in the friction stir welded copper to Al6061-T6.They found that nugget zone is composed from several intermetallic compounds; such as: $CuAl_2$,CuAl, Cu_9Al_4 and small amounts of α-Al phase. The authors concluded that friction stir welding of dissimilar Al alloys and Copper is complicated due the brittle nature of intermetallic compounds that formed inside the nugget zone.

Starting by a thin sheet of aluminum and copper, Galvão et al [25] analyzed the effects of tool design and working conditions on the material flow during FSW of alumni grade AA5083-H11 to copper. They observed that the relative location of material with respect to the advancing side of the tool as well the tool geometry have a significant effects on the shape of Al-Cu interaction regions and the intermetallic compounds formation. Xue et al [26], supported Galvão et al [26] observations when they studied the effect of FSW parameters on both micro structure and mechanical properties of AL1060 and commercial copper butt joints. They revealed that defect free joints occurred when the copper plate was placed in the advancing side with larger pin offset to the retreating side and high spindle speed. Also, they recommended that a thin, uniform and continuous intermetallic layer between Al1060 and Cu was significant for FSW of Al and Cu defect

free joints. Following the observations of Xue [26], Galvão et al [27], investigated the influence of tool shifting to the retreating side on the structure and morphology of dissimilar Al6082-T6 and Cu butt joint. They proved that tool offset is one of the most effective techniques to solve the problems of Al-Cu friction stir butt welding joints due its ability of forming a large amounts of intermetallic-rich structures thus it is influence the dissimilar joint strength. Their experiments were conducted at constant rotational and welding speed at five different offset positions. The authors have another work regarding the influence of shoulder design on the formation of the brittle structure in dissimilar friction stir welding of Al and Cu [28]. In this work, they noticed that different tool designs result to different structures and intermetallic compounds. Also, they found that, each shoulder geometry promoted the formation of specific intermetallic content and effect the surface finish. Their conclusion was that scrolled shoulder geometry results to a regular surface without a large amount of intermetallic compounds at stirring zone compared to the conical shoulder.

On the other hand, Esther et al [29], studied the influence of shoulder heat input on the properties of dissimilar friction stir welds of AA5754 and Copper C1100 considering 15 mm, 18 mm and 25 mm different shoulder diameters, spindle and welding speed were varied from 600 to 1200rpm and 50 to 300 mm/min, respectively with the aim of changing the amount of heat input, the observed that as the heat input increases joint electrical resistance increases too.

2.6 Modeling of FSW process

This section will review the modeling techniques that have been developed in order to study the FSW process of joining dissimilar materials. Researchers used different computational modeling methods, in order to understand the mechanisms that govern the material behavior during the joining process.

At the early stages of FSW modeling, research was focused on the heat transfer and thermal analysis of the process. The outputs of these models were predictions of temperature distribution around the work piece. Song and Koracevic [30], presented a 3-D heat transfer model for FSW, with a moving coordinate system. The authors used finite difference method (FDM) to solve Navier Stock's energy equation. Their model could simulate the heat transfer process, but they faced difficulty in determining the temperature distribution.

Sung et al [31], have constructed a 3D model to simulate both thermal and flow in friction stir welding using a commercial computational fluid dynamic code FLUENT. The work piece material chosen was aluminum, simulated as incompressible non-Newtonian fluid. The convection /conduction boundary conditions were used and temperature dependent properties were used in the thermal model. Heat generation by plastic deformation is considered from the sticking conditions between tool and plate was considered.

The material flow during FSW is complicated and directly influence the properties of welded joints It is affected by the tool design i.e. threaded conical pins could increase the

mixing as well as decreasing the process load. FSW process parameters and material to be weld are also considered factors which effect on the material flow. Thus, visualization of the flow during FSW is important for high quality weld and optimum tool design. Colegrove and Shercliff [32], modeled the 3-D metal flow in FSW by CFD using a standard threaded pin tool profile, their objective was to understand the material flow around a complex FSW tool and study the effect of process parameters. They found that material in line with the deformation zone was swept around the retreating side of the pin, where the amount of the material swept around the pin increases at a location closed to the shoulder. Also, they noticed that deformation zone size was much larger than that observed experimentally.

Thermo-mechanical modeling of FSW is important because of its capability to evaluate the stress and the strain as a result of the thermal gradient, In addition, the tool axial force, ignoring the metal flow in case of thermo-chemical modeling (non-flow based) or by considering it in case of thermo-mechanical (flow based) modeling or Arbitrary Lagrangian Eulerian (ALE).

Thermo-mechanical modeling of (non-flow based) FSW can predict the residual stresses that are produced as a result of thermal strain and the applied axial load which affect the strength of the joint after the process. Rajesh et.al [33], numerically determined residual stresses in friction stir welding by using 3-D analytical model of stir zone around the pin tool. They neglected the friction force during the steady state of FSW. Their justification was that the material in the stir zone is plasticized and it is plastically deformed rather than induced friction to the pin tool. They found that the maximum predicted longitudinal

residual stress component was 24% of material yield strength. Also, due to the symmetry in the plasticized material volume along the joint sides of the stir zone (that produced the heat), the residual stress distribution was symmetric.

Buffa et al [34], conducted extensive research work in the FSW field. They developed continuum based finite element model (FEM) 3-D Lagrangian implicit, coupled, rigid visco-plastic model of FSW. This model was calibrated with the experimental data of force and temperature distribution. The model explained the non-symmetry nature of the process as well as the relationship between the tool forces and the variation in the process parameters. While temperature distribution profile around the tool was found to be symmetric; the strain distribution was not. The maximum temperature and the maximum strain nugget decrease in the advancing speed. Moreover, the non-symmetric behavior of the deformation (material flow) in the weld zone is mainly controlled by both advancing and rotation speeds.

Recently available models [35, 37], are emphasized that the interaction between the rotation and advancing pin-shaped tool with the clamped welding plates, FSW processes must be studied numerically by using a fully coupled thermo-mechanical finite element analysis. Grinjici et al [35], used this technique in term of Arbitrary Lagrangian Eulerian (ALE) formulation to avoid the problem of extensive mesh distribution entanglement on the previous models [32,33,34,35]. ALE enables an adaptive remeshing – continuous high quality mesh that provides fully tracking of material-free surfaces. Material evolution during the friction stir welding of AA 5083 was predicted. Johnson – Cook strength model was modified to account for the effects of dynamic recrystallization and

the associated material softening around the stir zone of the welded joint. Their predictions showed good agreement with the experimental observations.

Al-Badour et al [36], presented a coupled Eulerian (CEL) model of the FSW to predict the conditions that caused the defect generation during the process. His work piece was modeled as an Eulerian domain where the tool was assumed as Lagrangian. Coulomb's friction contact model was adopted to define the interaction between tool and work piece and based on his numerical results. Coefficient of friction was found to have a major effect on void formation; whereas the lower the friction coefficient the larger the void formation tendency. It was also noticed that welding using force control at lower welding speed resulted in smaller void side and wider plastic zone, and lead to higher welding quality.

The preceding literature review reveals the fact that, in spite of its importance, only few authors attempted to experimentally study the process of welding aluminum to copper using FSW. In this work the friction stir welding process have been developed in order to achieve a sound butt joint of aluminum to copper. Finite elements models have also been used to simulate the joining process and study the effects of the process parameters on the weld features.

CHAPTER 3

Experimental Work

Friction stir butt weld tests were performed on 4 mm thick plates of measuring 100 mm × 50 mm along their length using the fully instrumented RM-1 FSW machine reported in Shuaib et al [5]. Three sets of welding tests were performed to join aluminum grade Al6061-T6 to aluminum grade Al6061-T6, commercial pure copper to commercial pure copper, and aluminum grade Al6061-T6 to commercially pure copper. The aluminum grade Al6061-T6 contains 97.56% Al, 0.91% Si, 0.84% Mg and 0.69% Mn with an average tensile strength of 131MPa whereas the commercial copper contains 99.65% Cu with an average tensile strength of 209 MPa. All tests used threaded pin tool made of H13 RC 50-55 steel with scrolled shoulder design, pin diameter of 5 mm, pin length of 3.7 mm, and shoulder diameter of 11.52 mm.

3.1 Friction Stir Butt Welding of Al6061-T6 to Al6061-T6

Joint welding condition was1100 rpm rotational speed and 175 mm/min feed rate. The tool was tilted by 3° during the experiment, where Figure 3.1 shows the friction stir butt welding of similar Al6061-T6. The joint quality `was evaluated by considering the Vicker's hardness across the welding direction and its tensile strength compare to the base metal, where, the joint was cut from the butt weldment according to the ASTM-E8 M [39] standard of sub size samples, Tensile tests w carried out on an Instron universal tensile test machine at rate of 2 mm/min ram speed by testing three different samples at

different positions where the hardness measuring condition was 300g load and 10 sec dwell time.

3.2 Friction Stir Butt Welding of Copper to Copper

The welds were performed at a constant tool rotational speed of 900 rpm where it is found from the literature review section that it is the speed of maximum tensile strength [21] and at four different welding speeds of 80, 100, 125 and 150 mm/min, FSW tool was tilted by 3° to increase the stirring area under the tool shoulder during the experiments. K–type thermo couple wires of 1 mm diameter sheath were mounted at a distance of 10 mm from the weld line and at 2 mm depth of the workpiece to measure the weldment temperature. The thermocouples were mounted at a distance of 10 mm away from the joint center to avoid its contact with the pin tool shoulder. The weld joints were evaluated first by examining their cross sections using an optical microscope and measuring their micro hardness across the weld beads. The metallographic specimens were prepared by sectioning, polishing, and etching in a solution that contains 1g of FeCl3, 10ml of HCl and 100ml of distilled water, to reveal the microstructure. Vicker's hardness readings were taken across the welding zone using 300 g load and 10 sec dwell time. Tensile specimens, used to evaluate the weldment strength, were cut from the butt weldments according to the ASTM-E8 M standard of sub size samples [37] as shown in figure 3.1. Tensile tests were carried out on an Instron universal tensile test machine type at rate of 2 mm/min ram speed.

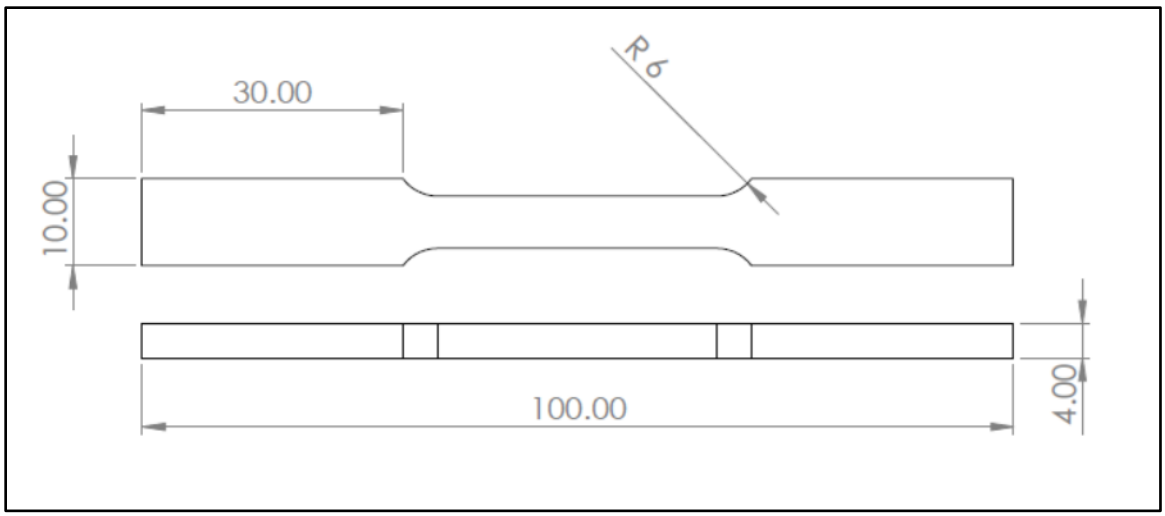

Fig. 3.1: ASTM-E8 M standard of sub size samples, in mm.

3.3 Friction Stir Butt Welding of Dissimilar Al6061-T6 to Copper

Pure commercial copper and Al6061-T6 plates measuring 100 mm × 50 mm × 4 mm were butt jointed using FSW process. Table 3.1 shows the welding conditions used in the investigation. The rotational speed of the tool was maintained at 900 rpm with 3° tilt angle for all test conditions. The material which was placed on the advancing side of the tool at each weld condition is shown in the last column of Table 3.1. All tests were performed on a fully instrumented experimental model RM-1 friction stir welder manufactured by MTI.

The weld beads were cross-sectioned, polished, and etched using a solution of one gram of FeCl3, 10 ml HCl, and 100 ml distilled water to reveal copper side microstructure first and then using a of 3 ml HNO3, 6 ml HCl, 6ml HF and 150 ml of distilled water to reveal the Al6061-T6 side microstructure. The weld joints were evaluated by examining

the optical microscope images of their cross sections to identify the presence or lack of voids, cracks and discontinuities. Using 300 g load and 10 sec dwell time, Vicker's hardness readings were taken across the weld nugget at two locations, 1.5 mm and 3.00 below the top surface of the plate. Energy dispersive spectroscopy (EDS) analysis was performed at various locations of the weld joint to identify the elemental distribution of copper and aluminum.

Table 3.1: Welding Parameters and Conditions

Test Condition	Welding Speed (mm/min)	Tool Offset (mm)	Advancing Side Material
1	150	0	Al6061-T6
2	40	2	Al6061-T6
3	40	2	Cu
4	20	0	Cu
5	40	0	Cu

CHAPTER 4

Finite Element Model of the Butt Weld Process

4.1 Coupled Eulerain Lagrangian (CEL) Model of Cu to Cu joint

4.1.1 Problem Idealization

A coupled Eulerian Lagrangian model was developed by Al-Badour et al [36] is modified in this work to simulate the FSW process of commercial pure copper. The model is implemented and solved in Abaqus environment using Explicit solver [38]. The workpiece is assumed as an Eulerian domain, while the FSW tool is considered as rigid Lagrangian body, constrained to specific reference point. Thus all physical properties and steps boundaries are assigned to this point.

4.1.2 Materials Model

The plastic flow of the commercial pure copper material used in this study is governed by the following Johnson-Cook's-empirical relation that correlates the relationship between the flow stress σ_o, strain rate έ and temperature T as shown on equation 4.1 [39].

$$\sigma_0 = (A + B\bar{\varepsilon}_{pl}^{n})\left(1 + C\ln\frac{\dot{\bar{\varepsilon}}_{pl}}{\dot{\varepsilon}_o}\right)\left(1 - \left(\frac{T - T_{ref}}{T_{melt} - T_{ref}}\right)^{m}\right) \quad (4.1)$$

where ε_{pl} is the effective plastic strain, $\dot{\bar{\varepsilon}}_{pl}$ the effective plastic strain rate, $\dot{\varepsilon}_0$ normalizing strain rate (typically 1.0 s-1), A, B, C are material constants, n parameters takes into account the effect of strain hardening, m models the thermal softening effect and C represents the strain rate sensitivity. T_{ref} is the temperature where A, B and n are

evaluated while T_{melt} represents material solidus temperature. For the CEL model all the elastic and thermal properties are taken as a function of temperature where 90% of the plastic work is assumed as plastic heat since the deformation caused at the materials plastic limits due to the stirring action of the tool. The constant of Johnson-Cook's-empirical law for copper are given in Table 4.1 [39].

Table 4.1: Copper Johnson-Cook's Parameters [39]

A (MPa)	B (MPa)	C	n	m	T_{ref} (K)	T_{melt} (K)
90	292	0.025	0.31	1.09	298	1356

4.1.3 Loads & Boundary Conditions

The interaction between the Eulerian and Lagrangian domains was coupled using general defined formulation of Coulomb's Law. The coefficient of friction μ is assumed to be 0.35 between steel and copper [40]. Assuming the velocity is constrained around the Eulerian domain, so the material will not escape.

In the FE simulation of this model, tool rotational speed and welding speed were taken as 900 rpm and 125 mm/min, respectively. Figure 4.1 shows a typical model mesh used in representing the Eulerian and Lagrangian domains.

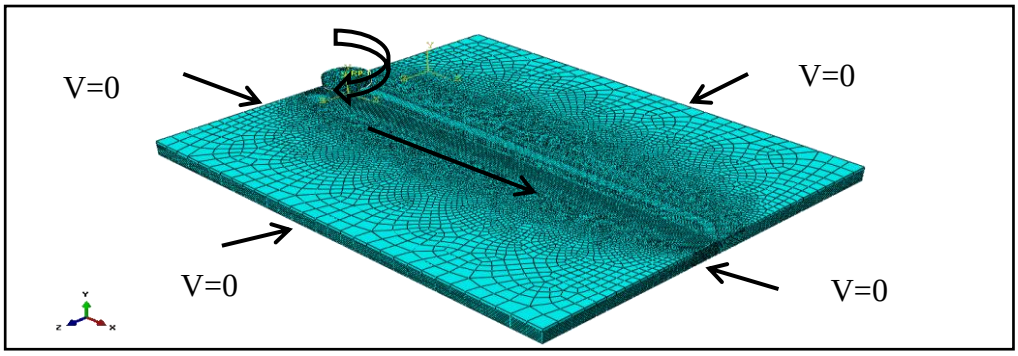

Fig. 4.1: Meshed Workpice (Eulerian Domain) and FSW Tool (Lagrangian Domain)

4.2 CEL Model of Pure Copper to Al6061-T6 Joint

4.2.1 Problem Definition

The coupled Eulerian Lagrangian model that has been developed in section 4.1 to simulate the FSW process of pure copper is modified here to simulate the FSW process of dissimilar Al606-T6 to Cu butt joint. This model is a modification of the one that was developed by Al-Badour et al [41], by considering a full geometrical model with threaded feature for the pin tool. The model is implemented and solved in Abaqus environment using explicit solver. The workpiece is represented by an Eulerian domain, while the FSW tool is considered to be rigid Lagrangian body that is constrained to specific reference point; thus all physical properties and steps boundaries are assigned to this point.

In the finite element model, an Eulerian domain dimensions were equal to those of the workpiece used in the experiment. The Eulerian domain was divided into three parts to define the advancing side, retreating side, and a void layer of 1mm thick added to the top of the Eulerian domain to help visualize the flash formation during welding. The pin has the material, dimensions, and features described in the experimental procedure section 3.1. Biased seeding was used to generate fine mesh in the weld seam line and coarse mesh at the edges in order to reduce the number of elements and reduce the computational time. Eulerian domain was meshed using multi-material thermally coupled Eulerian elements (EC3D8RT8), whereas coupled displacement temperature (C3D4T)

element type was considered for the Lagrangian domain, the mesh details are illustrated in Table 4.2.

Johnson-Cook's-empirical law [39], which considers the effects of strain hardening, strain rate, and temperature on material properties is used to represent the plastic flow σ_0 of copper and aluminum 6061-T6 as shown previously in equation 4.1, For the CEL model all the elastic and thermal properties are taken as a function of temperature and 90% of the plastic work is assumed as plastic heat. The values for modulus of elasticity, thermal conductivity, specific heat, and coefficient of thermal expansion are temperature dependent and were taken from materials property tables [41]. Johnson-Cook's-empirical law constants for aluminum grade Al6061-T6 are given in Table 4.3.

Table 4.2: Al6061-T6/Cu CEL Model Mesh Details

Part	Element Type	Element Shape	No. of Elements	No. of Nodes
Workpiece	EC3D8RT	Hexahedral	280852	307740
Threaded Pin Tool	C3D4T	Tetrahedral	57568	10991

Table 4.3: Al6061-T6 Johnson-Cook's Parameters [41]

A (MPa)	B (MPa)	C	n	m	T_{ref} (K)	T_{melt} (K)
324	114	0.002	0.42	1.34	298	855

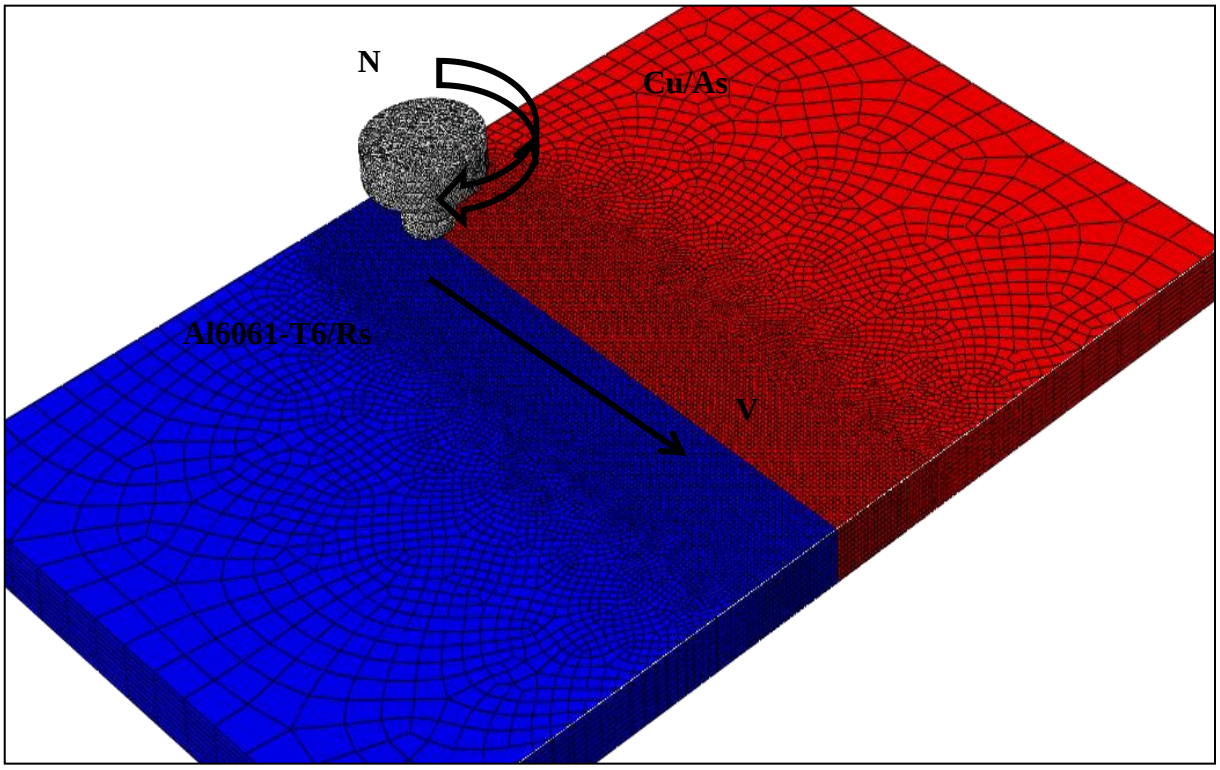

Fig. 4.2: Al6061-T6/Cu CEL mode materials locations and mesh generation

Coulomb's friction Law with an average coefficient of friction μ =0.5 was used to represent the interaction between the Eulerian (aluminum and copper) and Lagrangian (tool) domains [40]. As the Eulerian mesh is rigid, velocity constrains around the Eulerian domain were applied to avoid material escape. In the FE simulation model of joining aluminum 6061-T6 to copper, the tool rotational speed and welding speed were 900 rpm and 40 mm/min, respectively. Moreover, the effect of tool offset on the weld joint quality was studied using 0 mm, 1 mm and 2 mm offsets value to the retreating side. Figure 4.2 shows a typical model mesh of the Eulerian and Lagrangian domains.

CHAPTER 5

Results and Discussion

5.1 Friction Stir Welded Al6061-T6 to Al6061-T6 Butt Joints

5.1.1 Weld Strength and Hardness

The average tensile strength of the butt joint was 140 MPa with joint strength efficiency of 107 % greater than the base metal. The friction stir welding butt joint as welded is illustrated in Figure 5.1, where, Vicker's hardness results across the cross-section of weld bead were shown plotted in Figure 5.2. Stirring zone hardness results were higher than that on the base metal due to the process of grains refinement at this zone after welding. These results confirmed the findings obtained from the literature [41]. The joint tensile strength is greater in the weld nugget zone compare to the other welding zones, the explanation of that is the refining of the grains inside this zone due to the strain hardening.

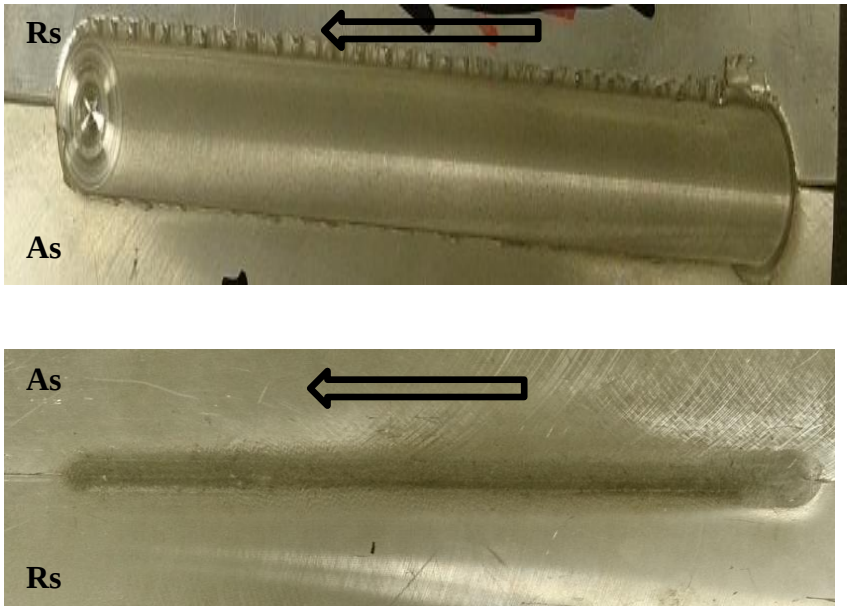

Fig. 5.1: Similar Al6061-T6 Butt Joint (V=175mm/min, N=1100rpm), Rs: Reterating Side and As: Advancing Side

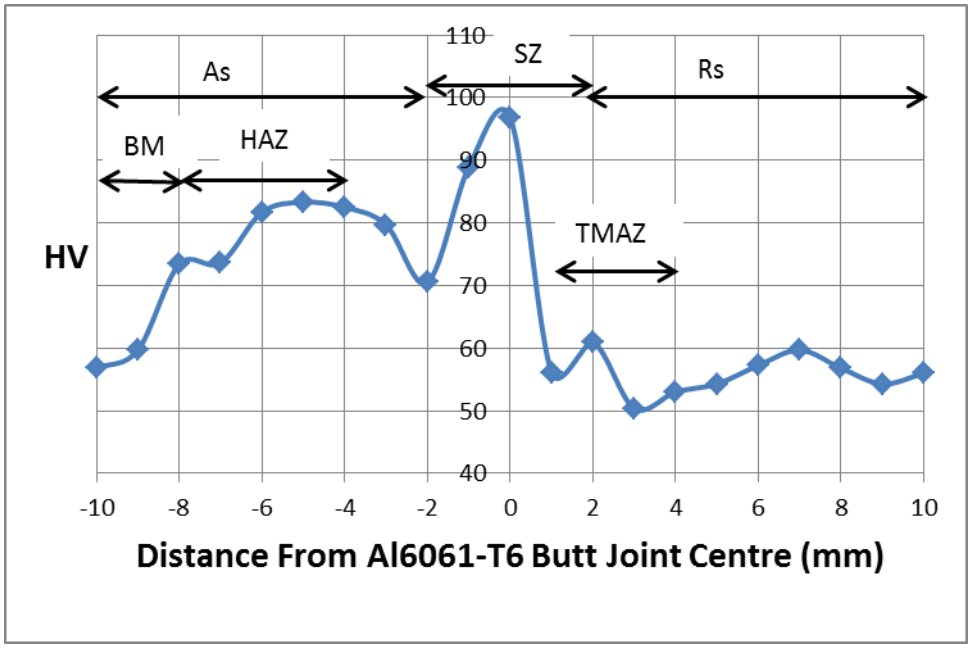

Fig. 5.2: Vicker's Hardness Distribution across Al6061-T6 Butt joint (V=175mm/min and N=1100rpm), (BM) Base Metal, (HAZ) Heat Affected Zone, (TMAZ) Thermo-Mechanical Affected Zone and (SZ) Stir Zone.

5.2 Friction Stir Welded Copper to Copper Butt Joints

5.2.1 Model Validation

Experimental temperature results measured during welding at a position of 10 mm away from the weld joint center explained previously in section 3.1.2 as well as corrrrospding measured axial force were used for validating the FE model results. Figure 5.3 shows that the measured axial pin tool force during the plunging phase and that estimated by the FE model are very close in value during the first 9 seconds. The deviation in the axial

force values after 9 seconds could be attributed to the contact of the pin tool shoulder towards the end of plunging where modified coulomb's law is more applicable due to sticking where by increasing the sticking the plunging force increases too. The measured temperature at 10 mm from the center of the tool was 623K while that estimated by the CEL model was 647.5K, i.e. a difference of 3.7% only.

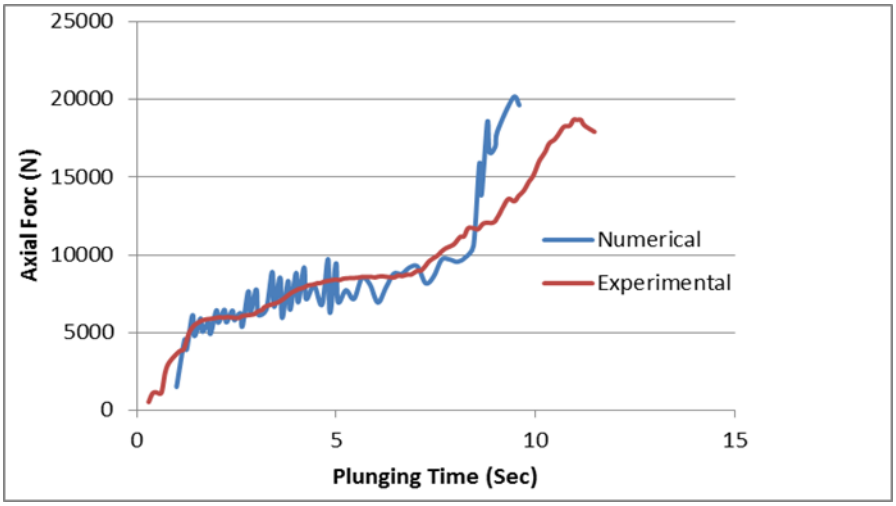

Fig. 5.3: Comparison of estimated tool axial force and measured one

5.2.2 Temperature Distribution across the Workpiece and Nugget

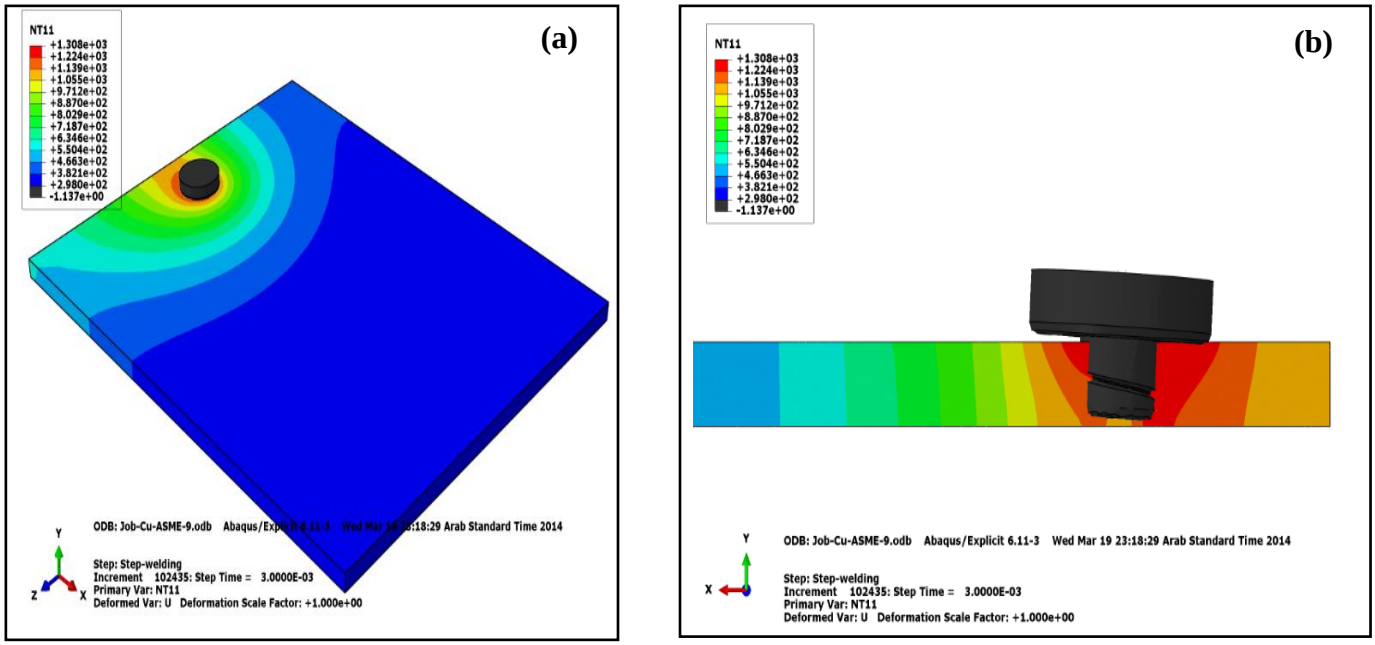

Fig. 5.4: Temperature Distributions at the Welding Stage (a) Top View and (b) Along the welding in Kelvien at 900rpm and 125mm/min.

Figure 5.4 (a) shows the top view of the steady state temperature distribution in the workpiece. The figure shows that temperature is higher at the retreating side of the pin tool compared to the advancing side [21]. Figure 5.4 (b) shows the temperature distribution in the workpiece along the welding direction. Both figures show that the maximum workpiece temperature is still below the copper melting point in the solidifying zone i.e. 80 % of the copper melting temperature and located close to the FSW tool [21].

5.2.3 Average Equivalent Plastic Strain (PEEQVAG)

Figure 5.5 shows the cross section of a sound weld bead made at tool rotation speed of 900 rpm and welding speed of 125 mm/min, which is superimposed on the CEL average

plastic strain distribution map. The figure shows the stir zone (SZ), thermo-mechanical affected zone (TMAZ), heat affected zone (HAZ) and base metal (BM) zones of the weld bead. The figure reveals that the stir zone basin shape is widened towards the workpiece top surface, as reported by Sakthivel et al [16].

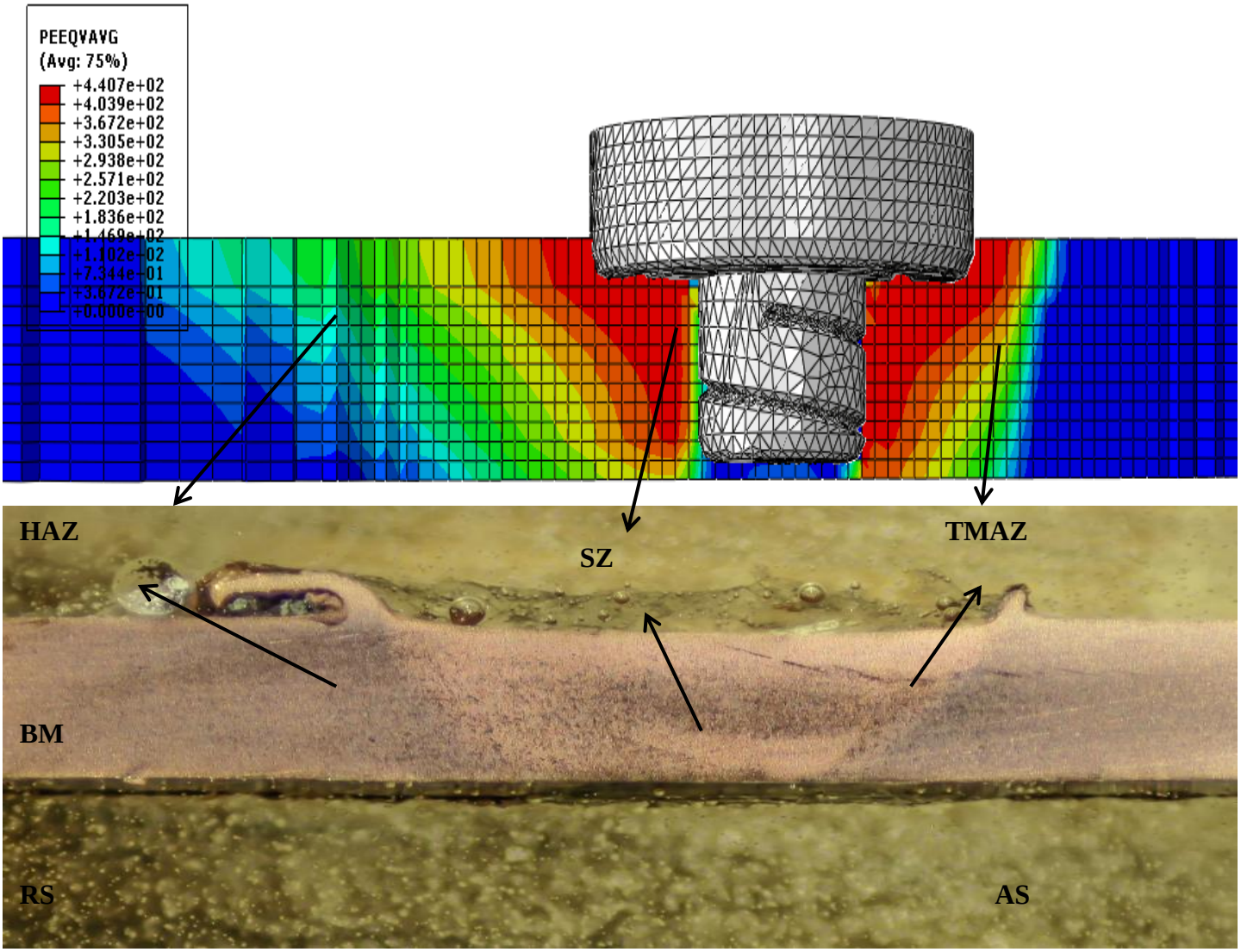

Fig. 5.5: Comparisons between the estimated plasticized zones, and revealed one, welding condition of 900rpm and 125mm/min

5.2.4 Weld Microstructure Zones

The effect of welding speed on the microstructure of the stir zone of the welded beads can be seen from Figure 5.6. The microstructure of the beads made at 80 mm/min, 100 mm/min, 125 mm/min, and 150 mm/min are shown in Figures 5.6 (a), (b), (c), and (d), respectively. Figure 5.7 shows that grain size of the stirring zone decrease with increasing the welding speed. This is attributed to the faster rate of cooling at lower levels of heat input. The manifestation of small grain size at higher welding speeds implies an improvement in the strength of the weldment, in spite of the limitations for this improvement [18].

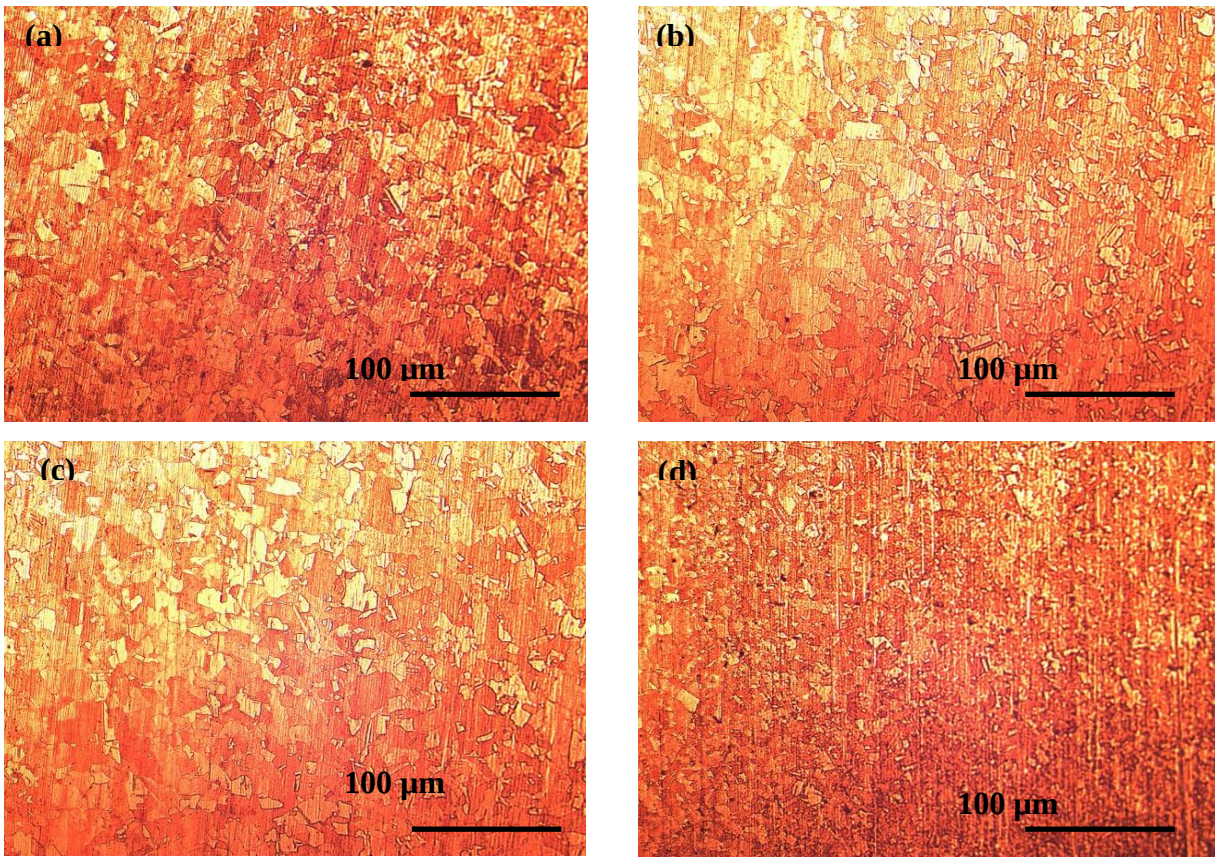

Fig. 5.6: Friction Stir Zone Microstructure at different welding speeds, (a) 80mm/min. (b) 100 mm/min. (c) 125mm/min and (d) 150mm/min.

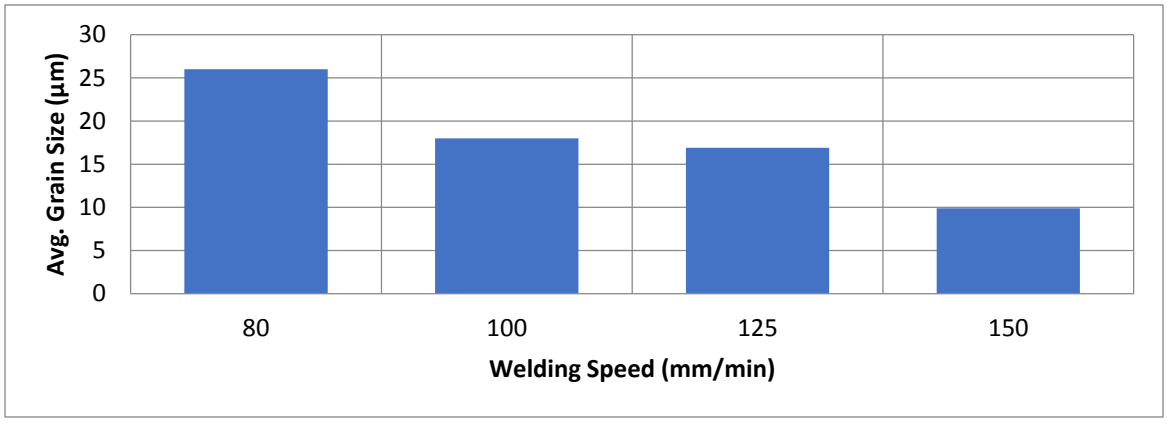

Fig. 5.7: Friction Stir Zone Average Grain Size at different welding speeds. (a) 80mm/min. (b)100 mm/min. (c)125mm/min.(d)150mm/min

Figure 5.8 shows the grain size across a weld bead made at pin tool speed of 900 rpm and welding speed of 150 mm/min depends at different weld zones. Figure 5.8 (a), (b), (c), and (d) correspond to the base metal (BM), heat affected zone (HAZ), thermo-mechanical affected zone (TMAZ), and stir zone (SZ), respectively. Figure 5.9 reveals that the grains are finer at the stir zone and progressively increase in size at the other zones towards the base metal. The existence of finer grains in the stir zone compared to the other zones is attributed to the grain refinement mechanism arising from the plastic deformation action of the pin tool on the workpiece.

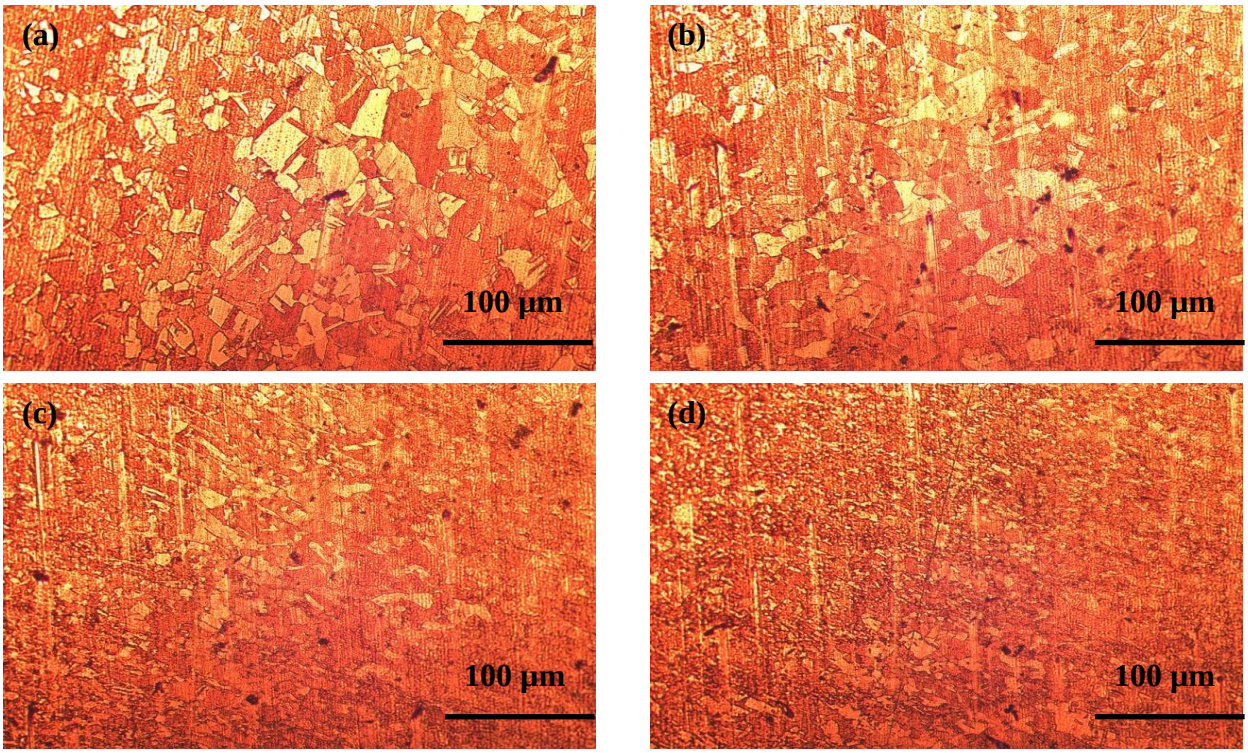

Fig. 5.8: Microstructure of (a) Base Metal, (b) HAZ, (C) TMAZ and (d) SZ at 900rpm rotational speed and150mm/min welding speed

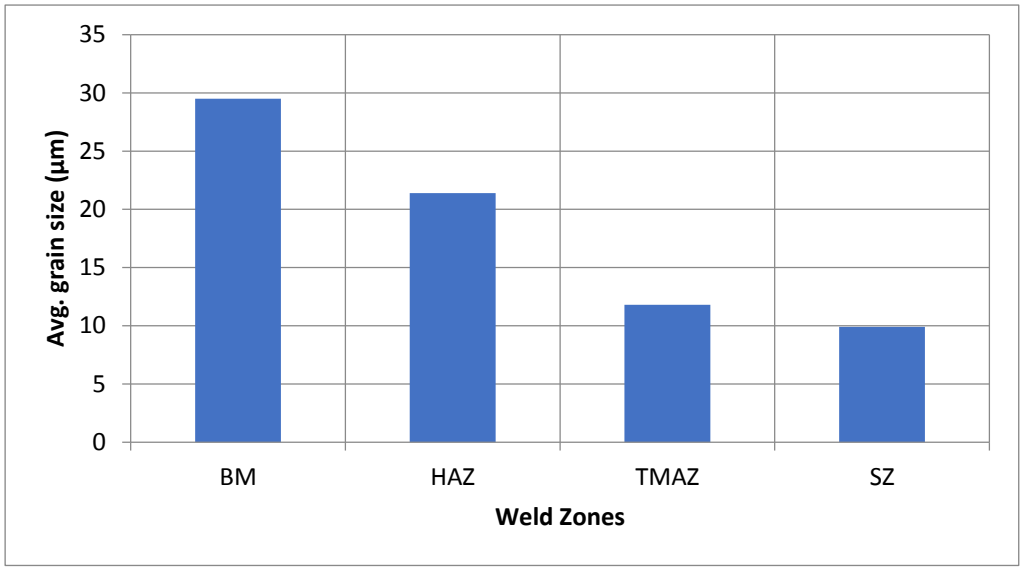

Fig. 5.9: Weld Zone Average Grain Size, (BM) Base Metal, (HAZ) Heat Affected Zone, (TMAZ) Thermo Mechanical Affected Zone and (SZ) Stir Zone, at 900rpm rotational speed and150mm/min welding speed

5.2.5 Weld bead Strength and Hardness

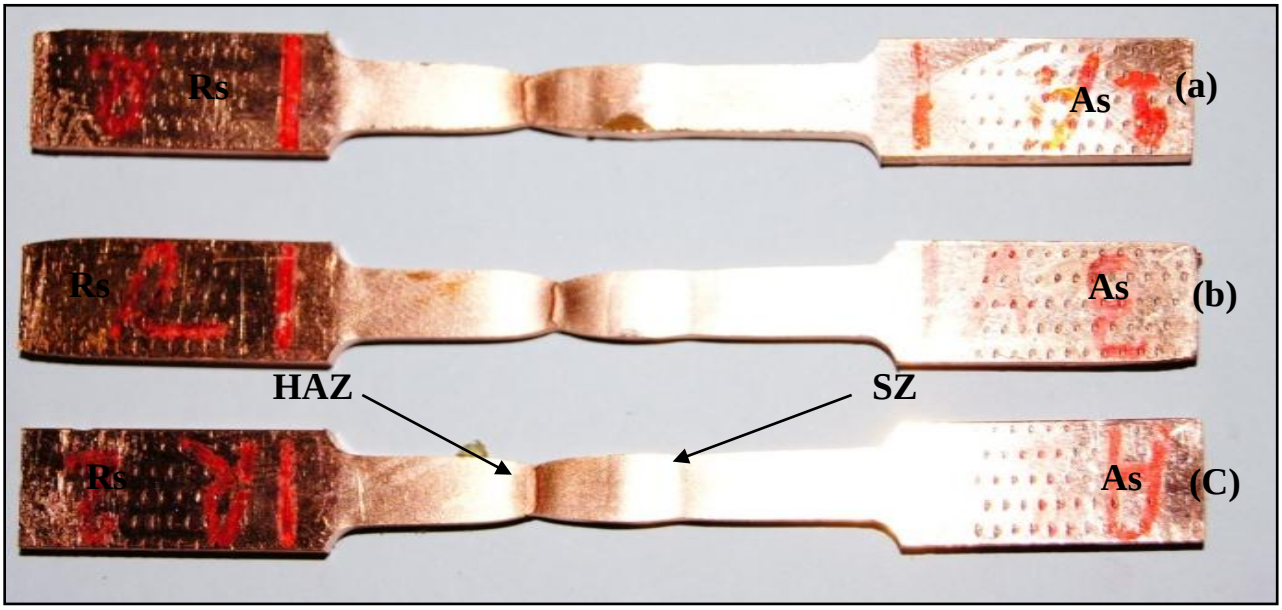

Fig. 5.10: Fracture Positions of Welded Products at Different Welding Speeds, (a) 150mm/min, (b)125mm/min and (c) 100mm/min.

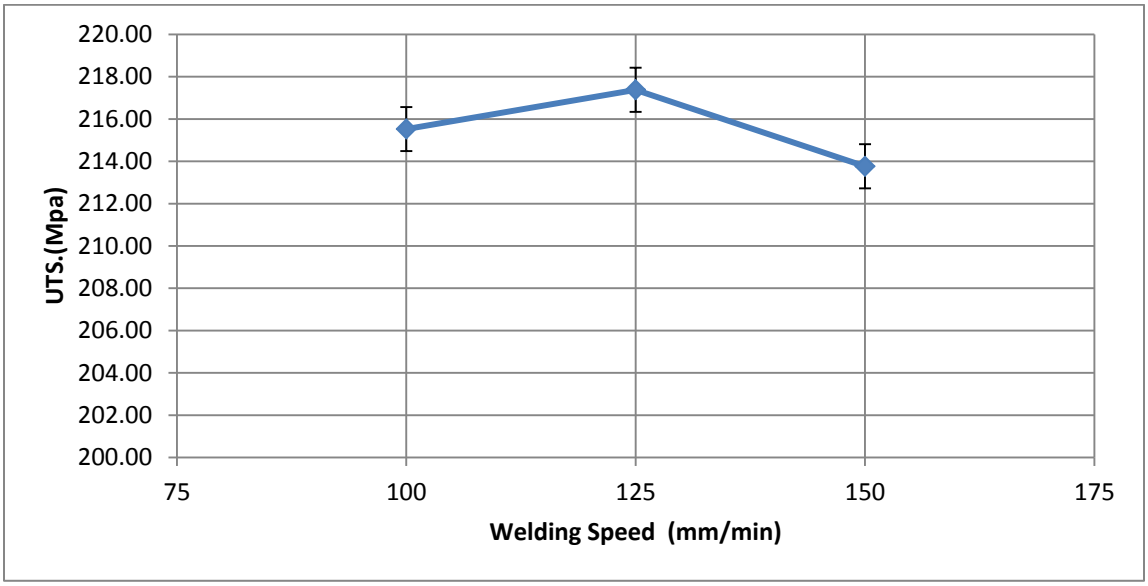

Fig. 5.11: Commercial Copper Butt Joints Tensile Properties at Different Welding Speeds

The effect of welding speed on the strength of the weld bead is obtained from the tensile tests. Figure 5.10 shows the fractures test specimens whereas Figure 5.11 shows the values of the strengths of the weld beads made by welding speeds of 100, 125, and 150 mm/min. The strength of the weld beads stir zone was found to be higher than the strength both heat affected zone and thermo-mechanical affected zone, where, the strength of the bead made at 125 mm/min was found to be the highest, and the scatter bars of the data appear to overlap.

Vickers hardness results across the cross-sections of 900 rpm rotational speed and 125 mm/min traverse speed weld bead is shown plotted in Figure 5.12. The figure shows that the stirring zone hardness is higher than that of the base metal. This is attributed to the presence of smaller grains at the stirring zone compared to larger grains at the other zones. Taking into account, the tensile strength and hardness data, it seems that the presence of the finer grains in the stir zone results to higher mechanical strength inside this region compare to the other weld zones.

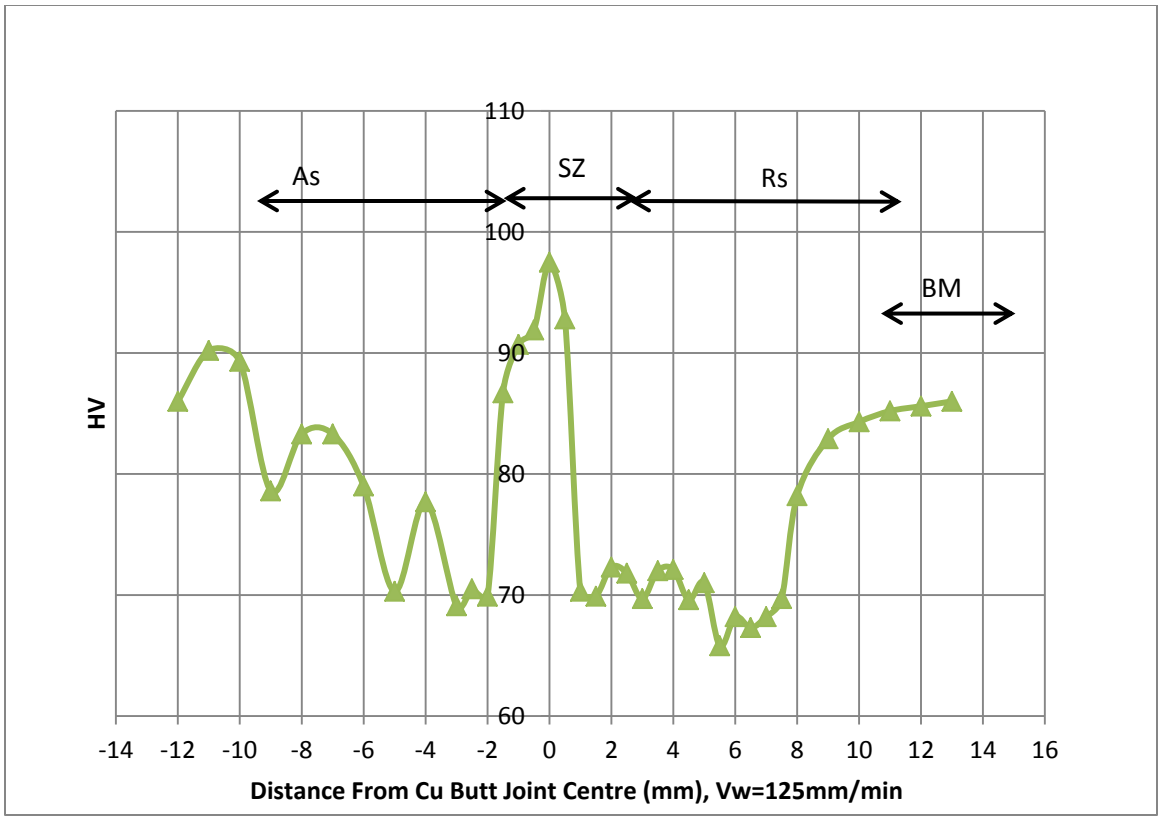

Fig. 5.12: Vickers Micro Hardness distributions at 125mm/min Welding Speed and 900 rpm rotational speed.

5.3 Friction Stir Welded Al6061-T6 to Copper Butt Joints

5.3.1 Finding Sound Weldment Conditions

This section covers the procedure for finding the friction stir welding conditions that produce defect free weldments of aluminum to copper butt joint. Welding tests were first conducted to identify the FSW parameters that produced sound weld joint for each of aluminum grade Al6061-T6 to aluminum grade Al6061-T6 and welding copper to copper as shown on the in sections 5.1 and 5.2, respectively. The goal is to use the results of these tests to find starting process parameters for welding aluminum to copper tests.

Defect free weld joints of Al6061-T6 to Al6061-T6 were obtained when welding was performed at tool rotation speed of 900 rpm, welding speed of 175 mm/min, plunging depth of 3.8 mm, and tool tilt angle of 3°. Likewise, the welding parameters for obtaining Cu to Cu sound weldments were found to be 900 rpm rotational speed, 125 mm/min welding speed, 3.8mm plunging depth, and 3° tool tilt angle. These optimum process parameters of welding copper to copper and aluminum to aluminum have been used as initial parameters for welding aluminum to copper.

The first trial test for welding aluminum to copper used the test condition 1 in Table 3.1 in section 3.1.3. The 150 mm/min welding speed of this condition is the average value of the welding speeds used in joining copper-to-copper and aluminum-to-aluminum. No welding was achieved during the first test condition and the tool pin failed by fracture after travelling 50 mm only. The tool failure is attributed to excessive force that overloaded the tool as shown by the force profile in Figure 5.13 (a). The figure reveals that during welding and prior to fracture, the cross feed force (traverse force) was very high and reached 7kN. The increase in traverse force was caused by less softening of copper due to the fast cooling rate, that led to low heat generation, when welding at the high welding speed of 150 mm/min. In order to avoid tool failure and to obtain sound weld quality, several trials were performed under lower welding speed conditions of 80, 40, and 20 mm/min. Furthermore, the effect of having the softer material (aluminum) or the harder material (copper) at the advancing side of the tool and of using tool offset relative to the center of the weld bead was explored at these welding speeds. It was

possible to identify the conditions which resulted in lower welding forces and acceptable weldment quality.

Figure 5.13 (b) shows the profile of the cross feed force on the tool when copper was placed at the advancing side, the rotational speed of tool was 900 rpm, the welding speed was 40 mm/min, penetration depth was 3.78 mm, the tilt angle was 3^0, and zero offset. Similarly, Figure 5.13 (c) shows the profile of the cross feed force on the tool using the welding conditions of Figure 5.13 (b), except the copper was placed in the retreating side of the tool in addition to a 2 mm offset of the tool towards the retreating side. Likewise, Figure 5.13 (d) shows the profile of the cross feed force on the tool using the welding conditions of Figure 5.13 (c), except the copper was placed in the advanced side of the tool. We can now conclude from the results of Figure 5.13 that decreasing welding speed, placing the hard material on the advancing side, and using a 2 mm offset of the tool leads to lower welding forces. However, placing copper at the retreating side leads to higher forces even with the presence of an offset.

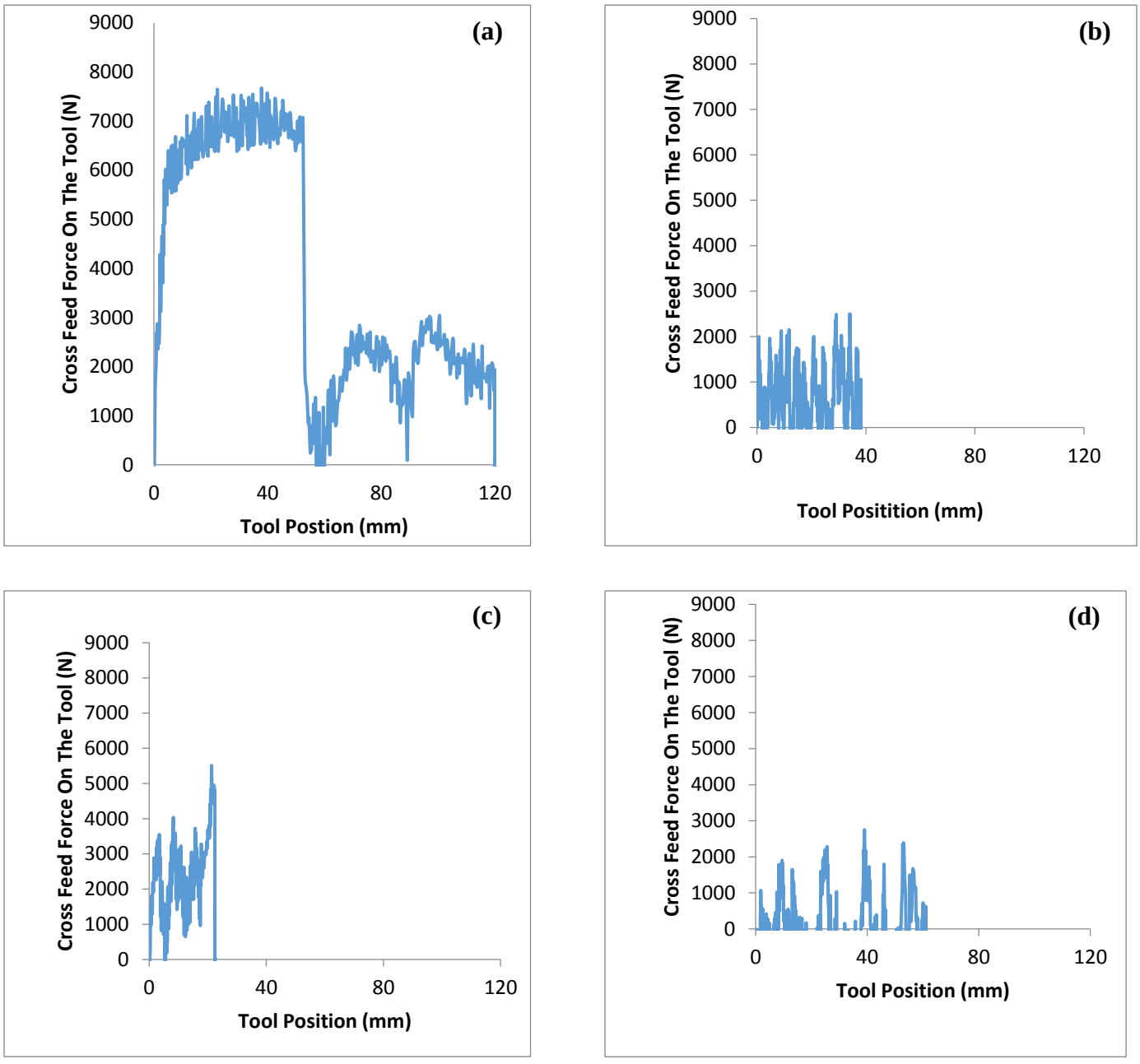

Fig. 5.13: Cross feed force profile vs welding distance on the tool at welding (a) condition1 (b) condition 4 (c) condition 2, (d) condition 3.

5.3.2 Characterization of Copper-Al6061-T6 Friction Stir Butt Welded Joint

The quality of the weld joints made on the weld conditions table 3.1, were evaluated by examining the optical microscope images of their cross sections to identify the presence or lack of voids, cracks and discontinuities. Figure 5.14 reveals the appearance of the sectioned, polished, and etched weldments of aluminum grade Al6061-T6 to copper at four different welding conditions. Figures 5.14 (a) and (b) exhibit voids in their weldments. Copper was placed at the advancing side for the weldment in Figure 5.14 (a) which was welded using tool rotational speed of 900 rpm, welding speed of 20 mm/min, penetration depth of 3.78 mm, the tilt angle was 3º, and zero offset. The conditions for making the weldment shown in Figure 5.14 (b) are the same as those of Figure 5.14 (a), except the welding speed was 40 mm/min. The lack of tool offset under these two conditions appears to be the reason for presence of voids.

Evidence of presence of cracks appeared in a magnified image of the weldment of Figure 5.14 (c). The weldment was made when Al6061-T6 was placed on the advanced side and using welding tool rotational speed of 900 rpm, welding speed of 40 mm/min, penetration depth of 3.78 mm, tilt angle of 3º, and 2 mm tool offset from the centerline of the nugget towards the retreating side of the tool. This leads to the conclusion that placing the softer material on the advance side produces defects. Figure 5.14 (d) shows aluminum to copper weldment with no defects. This weldment was produced at the same welding conditions of Figure 5.14 (c), except that the harder copper material was placed at the advancing side of the tool where more heat is generated by the tool compared with the retreating side. This provides copper with enough heat to soften it and the same time compensate

for the heat loss arising from the higher thermal conductivity of copper. The relatively lower amount of heat generation when Al6061-T6 was placed on the retreating side allows it to be softened below melting point. We can now conclude from the preceding results that it is possible to weld copper to Al6061-T6 and obtain sound weldment with relatively low welding force when copper is placed at the advancing side of the tool and using tool offset of 2 mm towards the retreating side.

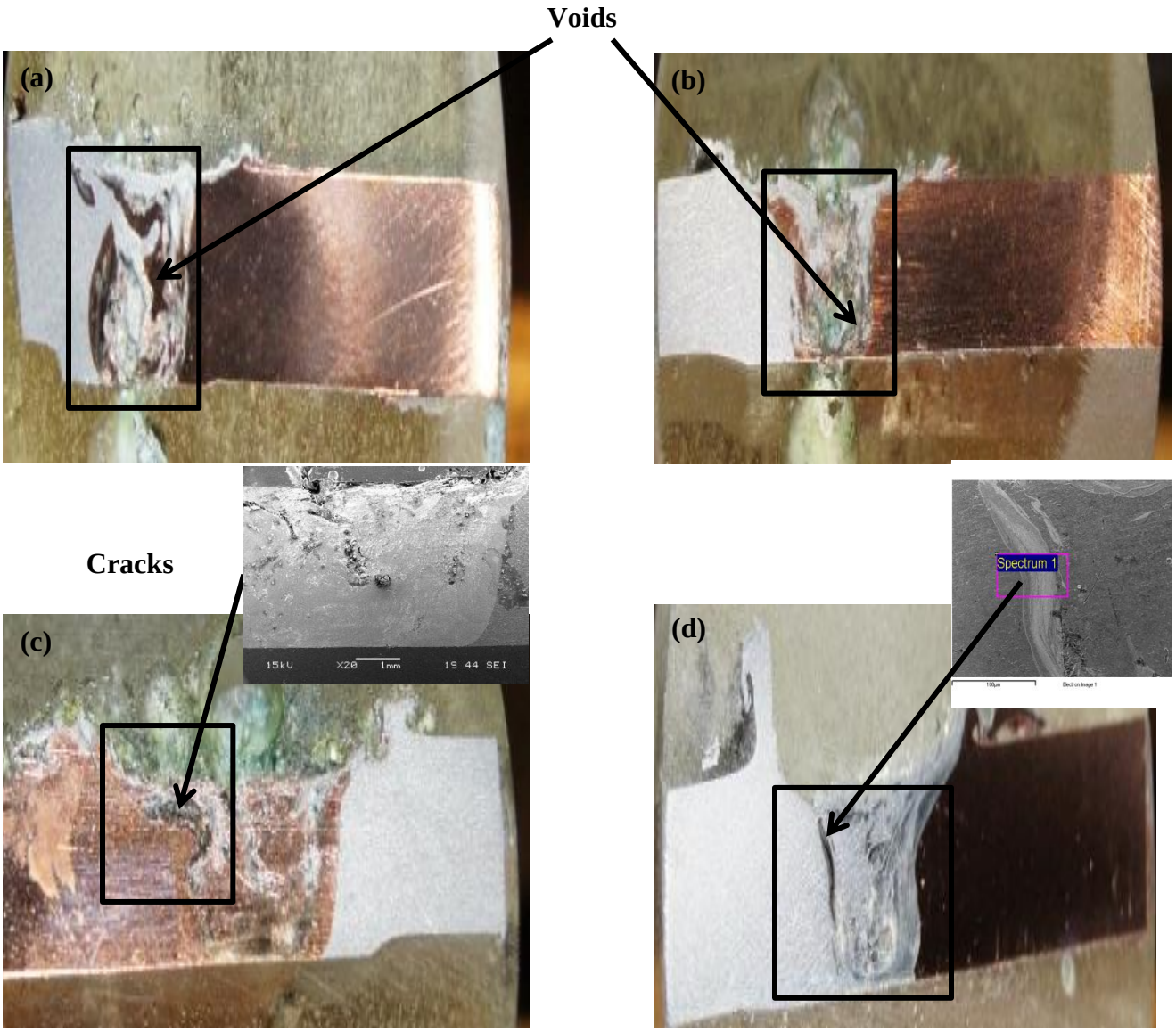

Fig. 5.14: Cross section macrostructure of dissimilar Al6061-T6/Cu and voids formation at different welding Conditions, (a) condition 4, (b) condition 5, (c) condition 3, (d) condition 2.

- **Weld Quality of Copper-Al6061 Interface Region**

The quality of the copper to Al6061-T6 weldments can further be assessed when their interfaces are examined from the respective optical images. Figures 5.15 (a), (b), (c), and (d) show optical images of the weldments corresponding to the weldments in Figures 5.15 (a), (b), (c), and (d), respectively. Close examinations of the former figures reveal formation of cracks at the interfaces between copper and the weld nugget for weld conditions of the weldments corresponding to Figures 5.14 (a), (b), (c), which had voids and cracks. On the other hand, Figure 5.15 (d) copper-weld nugget interface corresponding to the sound weldment shown in Figure 5.14 (d) is free of cracks. Energy dispersive spectroscopy (EDS) analysis performed on the interface of the sound weld revealed the presence of Al_2Cu intermetallic compound of composition 71.0 wt. % of Al and 29.0 wt.% of Cu.

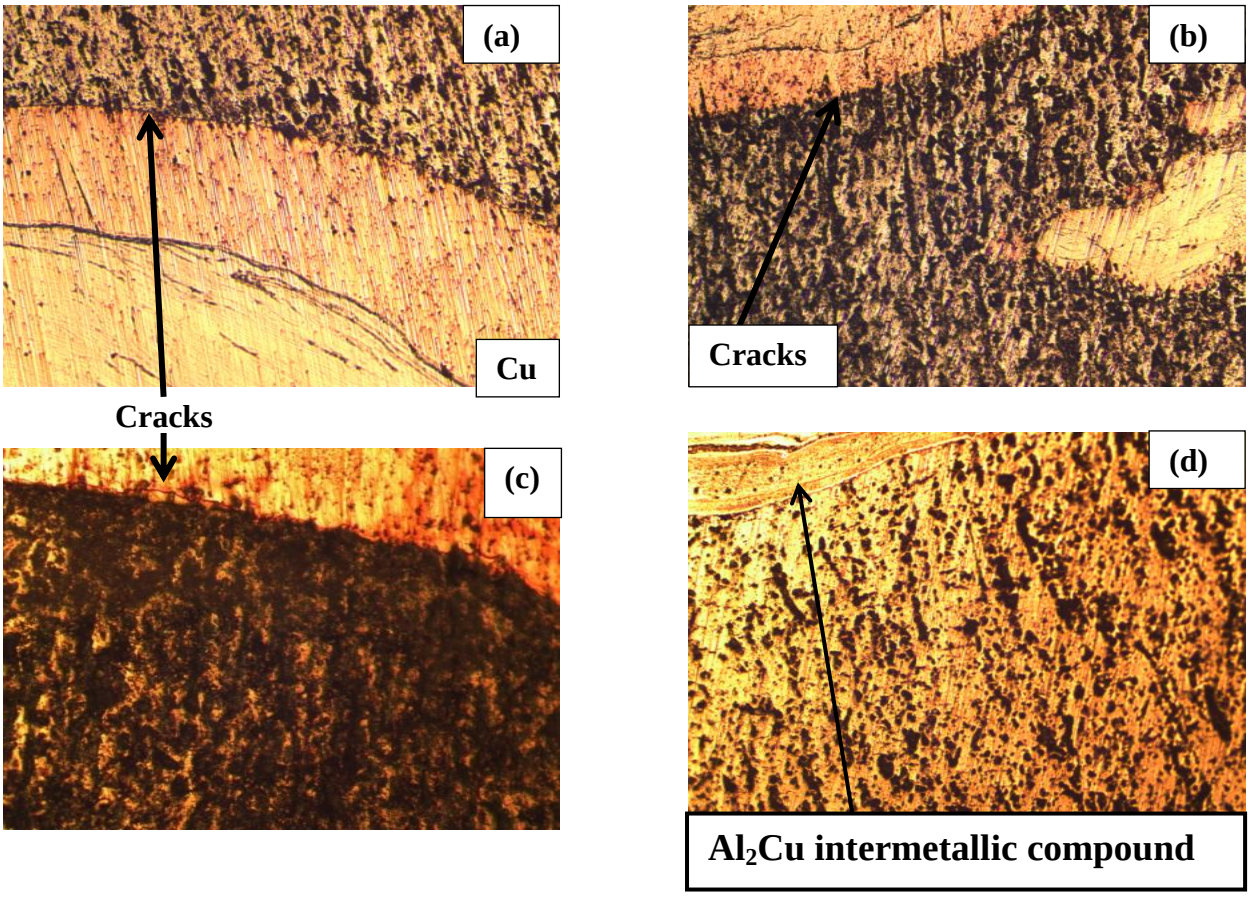

Fig. 5.15: Interface region micro structure of Al6061/Cu at different welding conditions, , (a) condition 4, (b) condition 5, (c) condition 2, (d) condition 3.

- **Phases in the copper-to-aluminum sound weld nugget**

The approach to identifying the phases present in the aluminum to copper wed joint nugget is to utilize the following:

1. Elemental composition and relative concentrations of aluminum and copper at various locations of nugget using EDS analysis
2. The temperature distribution of the weld nugget obtained from the finite element model

3. Phases and intermetallic compounds from Cu-Al phase diagram at various compositions and temperatures.

For example, to identify the present phase or intermetallic compound at a certain location of the nugget, find the concentration of Cu and its ratio to aluminum using EDS analysis, find the temperature at the location, and then use the phase diagram of Al-Cu to identify the phase at that location. This process is repeated for all points of interest. Figure 5.16 (a) shows the temperate distribution within the weld joint obtained from the finite element model and Figure 5.16 (b) shows the sound aluminum to copper weld joint together with some locations where EDS analysis were performed. The aluminum copper phase diagram is shown in Figure 5.17. The concentrations of copper and aluminum where EDS analyses were performed are shown in Table 5.1, together with the corresponding intermetallic phases present in the copper side of the sound aluminum to copper weld nugget; and Table 5.2 is for the aluminum side. The elements and phases present on the copper side of the nugget include single phases of Al_2Cu, AlCu, Al_4Cu_9, and Solid Solution Al (Cu) in addition to a two phase (Al+ Al_2Cu). Similar phases were also identified on the aluminum side of the sound nugget as shown Table 5.2.

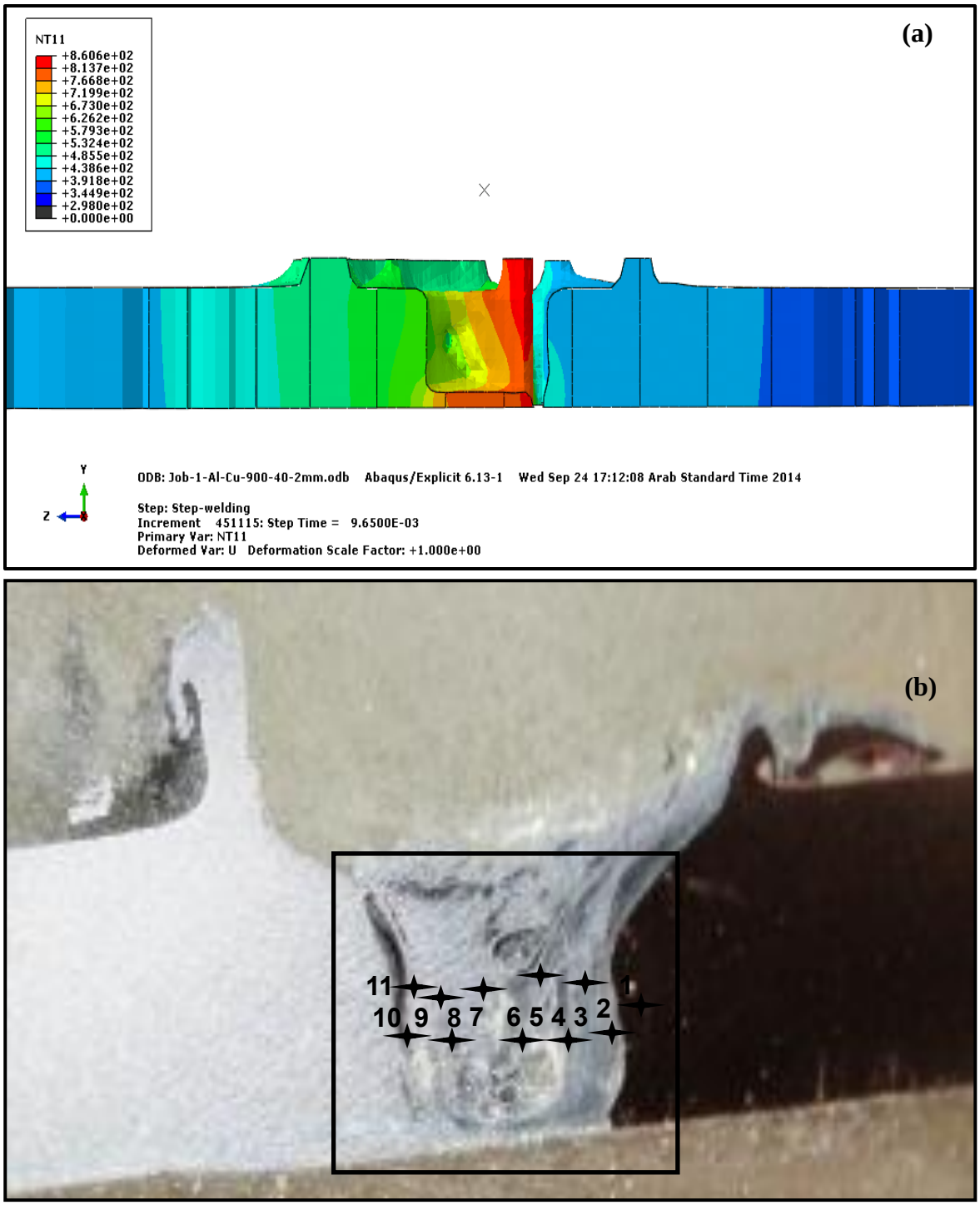

Fig. 5.16: EDS analysis locations at the sound weld nugget, condition 3

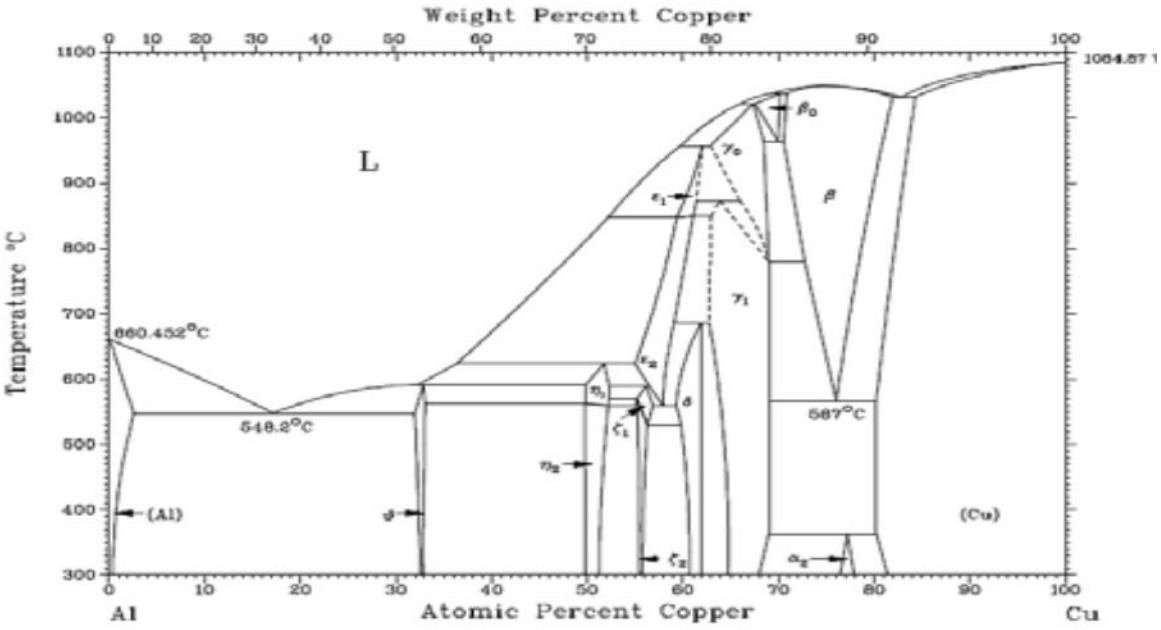

Fig. 5.17: Phase diagram of Cu-Al system [42]

Table 5.1: Spectrum analysis toward Cu side

Spectrum Location	Al, Wt.%	Cu, Wt.%	Possible Phase
1	69.55	30.45	Al_2Cu
2	76.17	23.14	Al_2Cu
3	92.87	6.36	Solid Solution Al (Cu)
4	86.74	12.46	Al+ Al_2Cu
5	84.31	14.95	Al+ Al_2Cu
6	75.23	24.04	Al_2Cu
7	67.1	32.05	Al_2Cu
8	72.05	27.23	Al_2Cu
9	82.33	16.89	Al+ Al_2Cu
10	52.66	46.75	AlCu
11	29.78	70.22	Al_4Cu_9

Table 5.2: Spectrum analysis towardAl6061-T6 side

Spectrum Location	Al Wt.%	Cu Wt.%	Possible Phase
1	94.44	4.75	Solid Solution Al (Cu)
2	19.05	80.95	Al_4Cu_9
3	90.89	6.78	Solid Solution Al (Cu)
4	93.54	5.65	Solid Solution Al (Cu)
5	64.32	34.96	Al_2Cu
6	93.72	5.35	Solid Solution Al (Cu)
7	71.71	27.62	Al_2Cu
8	61.30	37.85	Al_2Cu
9	55.38	44.62	AlCu

- **Hardness of the Copper-to-Aluminum weld Joints**

The general trend of hardness profile for Al6061-T6/Cu FSW butt joint is that hardness values are greater at the copper side interface compared to both aluminum side interface and weld nugget zone. Aluminum base metal hardness values vary between 47.8 HV to 68 HV, while copper matrix hardness readings vary between 78.4 HV to 97 HV. Figures 5.18(a) and (b) show Vickers's microhardness test results for aluminum to copper joints when the hard material at the advancing side, with no tool offset, and for welding speeds of 20 and 40 mm/min, respectively. Peak values were observed at the interface zone in copper side. At the bottom region of the interface zone as illustrated in Figure 5.18 (a),

microhardness was 191.4 HV. Considering similar location, 323 HV was measured when tool rotational speed was increased to 40 mm/min as in figure 5.18 (b). These two peaks are due to the intermetallic compounds formation inside these regions. Phases of AlCu as well as Al_2Cu_3 were detected previously by the EDS analysis and these phases have brittle and hard nature compare to copper base metal [40]. Likewise, these peaks were also found at the top of stir zone, for welds performed with tool offset. From Figure 5.18 (c) and (d), peak value of 261.7 HV was measured at test condition 2 of Table 3.1, while 240.4 HV is the peak value for test condition 3 as shown in figure 5.18 (d). Figure 5.18 (c) and (d) reveal that hardness profile fluctuation was less when tool offset technique was used, which was brought by the regular distribution of Al/Cu phases, Al_2Cu and Cu(Al) solid solution.

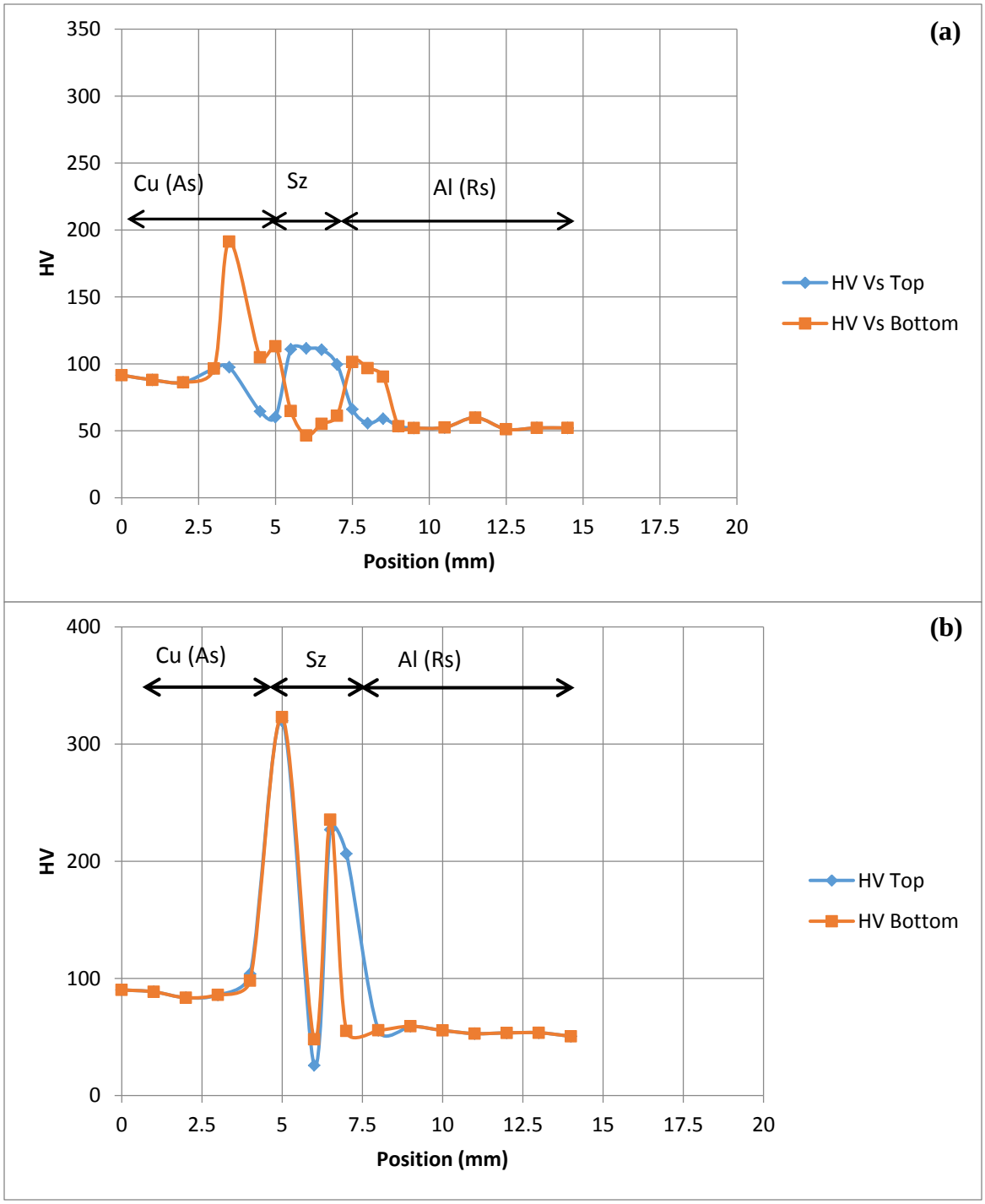
(a)
350
300
250
200
150
100
50
0
HV
Cu (As)
Sz
Al (Rs)
0
2.5
5
7.5
10
12.5
15
17.5
20
Position (mm)
HV Vs Top
HV Vs Bottom
(b)
400
300
200
100
0
HV
Cu (As)
Sz
Al (Rs)
0
2.5
5
7.5
10
12.5
15
17.5
20
Position (mm)
HV Top
HV Bottom

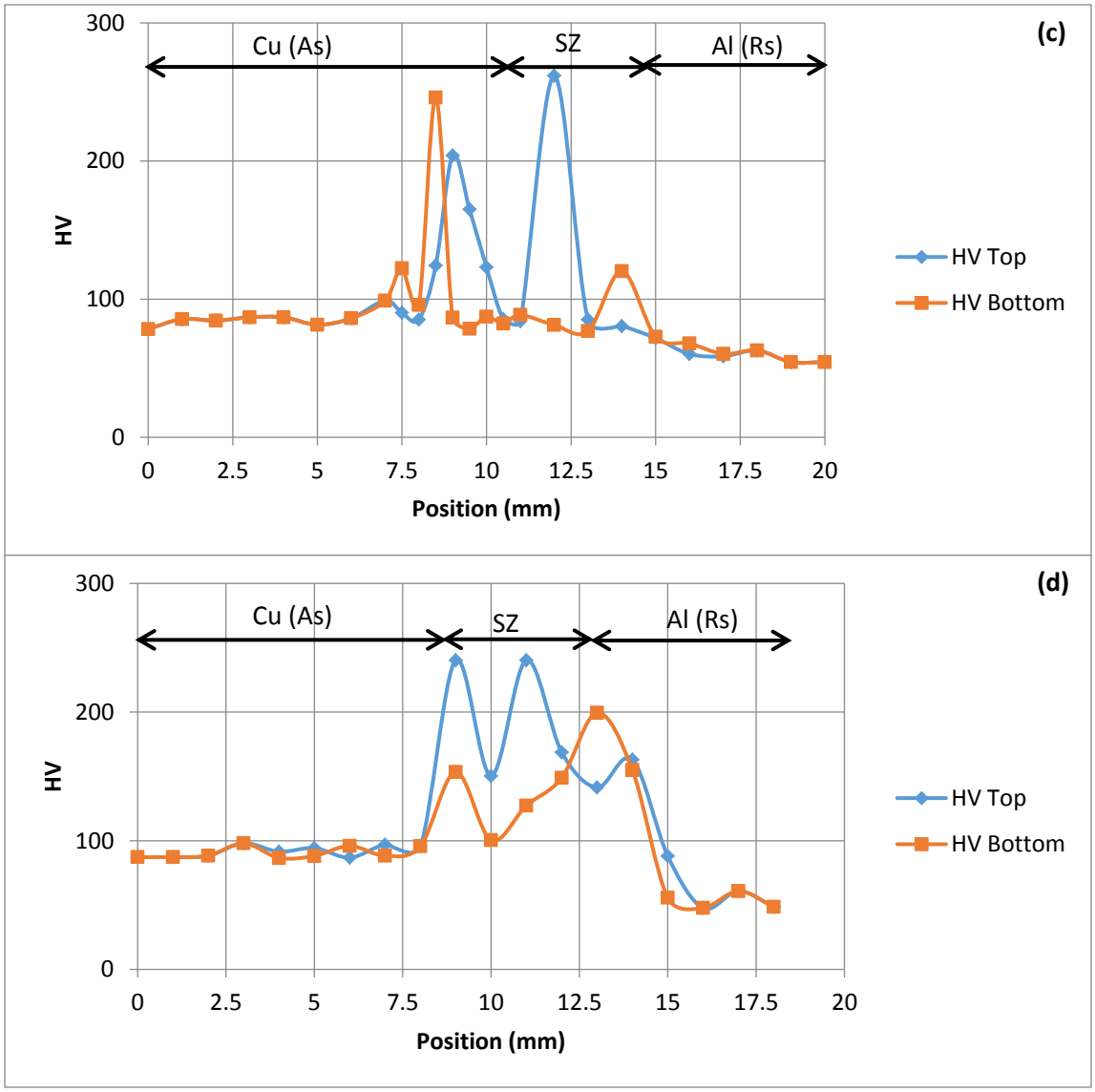

Fig. 5.18: Vickers Micro Hardness distributions at different Welding Conditions of Al6061-T6 and Cu FSW Butt joint, (a) condition 4, (b) condition 5, (c) condition 2, (d) condition 3.

5.3.3 Effect of tool offset on stir zone temperature distribution

Tool offset influence on stir zone temperature distribution can be deduced from Figure 5.19, where, considerable change in the temperature profile occurs by offsetting the tool by 2 mm towards the aluminum side, see Figure 5.19 (c). In this case higher and more regular thermal distribution were obtained compared to 0 mm and 1mm tool offset as shown on figure 5.19 (a) and (b) respectively. This regularity can explain the appearance of AlCu intermetallic compound in the stir zone by 2 mm offset as illustrated previously. Generally, temperature results are greater on the aluminum side compare to the copper side [24] because copper thermal conductivity is twice the aluminum thermal conductivity thus copper plate dissipates the heat two times faster than aluminum plates.

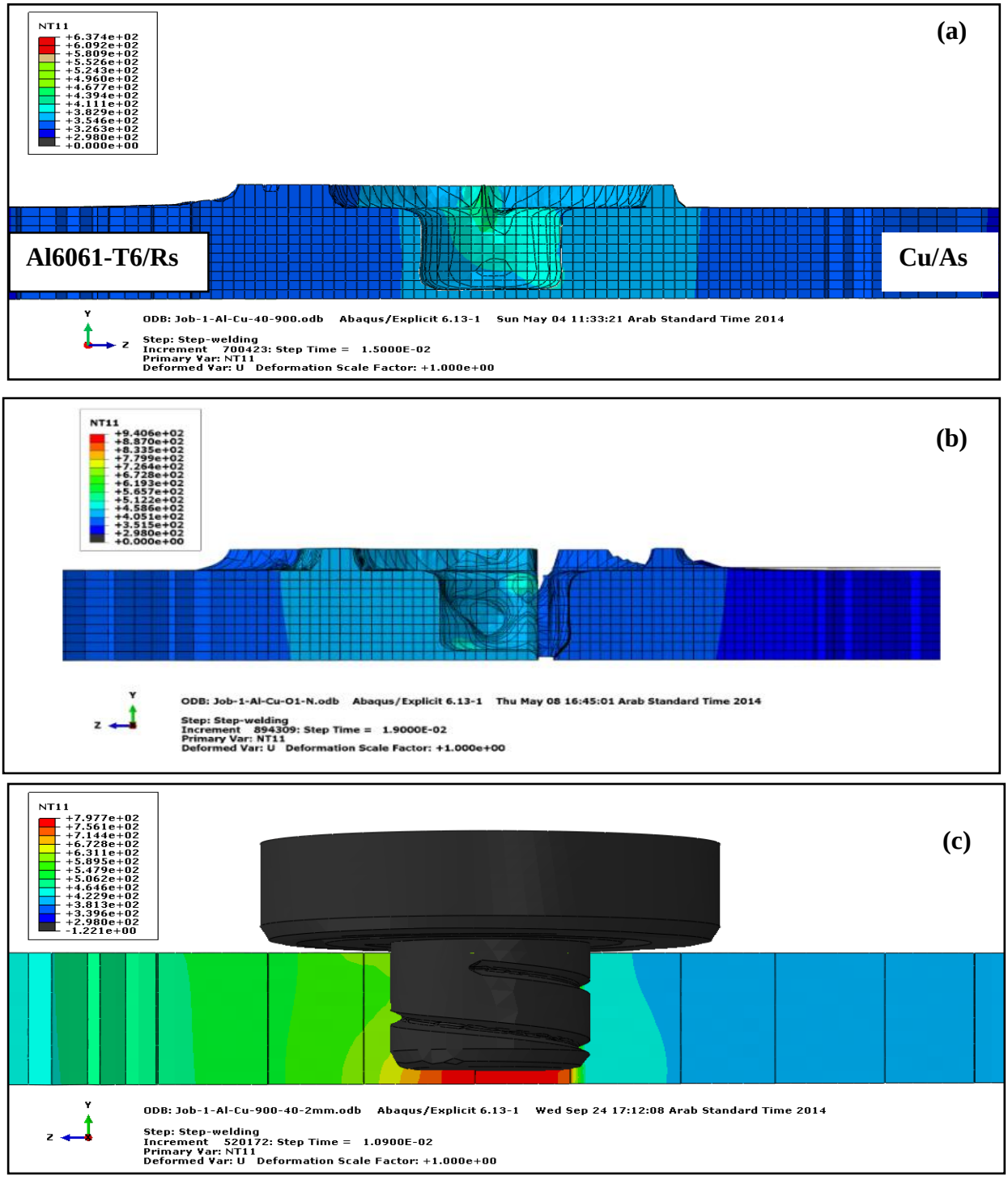

Fig. 5.19: Cross View of Temperature Distribution at Different welding conditions, (a) 900rpm, 40mm/min and 0mm offset, (b) 900rpm, 40mm/min and 1mm offset and (c) 900rpm, 40mm/min and 2mm offset

CHAPTER 6

Conclusions and Recommendations

6.1 Conclusions

In this work friction stir welding of selected aluminum grade Al6061-T6 to aluminum grade Al6061-T6, copper to copper and dissimilar aluminum grade Al6061-T6 to copper were investigated using experimental and numerical approaches and the friction stir welding conditions that resulted in sound weld quality were identified. The effect of FSW process parameters is studied by considering different welding speed, different materials location as well as different tool offsets to the retreating side. All welds were friction stir butt joints at constant rotation speed and tool tilt angle.

The following specific conclusions are drawn from the results of the study:

For aluminum to aluminum FSW butt joint:

1. Defect free joints are achieved at 1100 rpm rotational speed and 175 mm/min welding speed
2. The average tensile strength of the butt joint was 140 MPa with joint strength efficiency of 107 % greater than that of the base metal.
3. Vicker's hardness at the stirring zone were higher than that on the base metal due to the process of grains refinement at this zone after welding reported peak on the stir zone was 98 HV.

For copper to copper FSW butt joint:

1. It has been found that increasing the welding speed decreases the grain size thus affecting the joint mechanical properties.
2. The grain size in the stirring zone is smaller than that of the other zones.
3. The tensile tests showed that the weld bead strength is higher than the base metal, i.e. an efficiency that exceeds 100%.
4. The hardness in the stirring zone is higher than that of the base metal.

For the dissimilar aluminum to copper FSW butt joints:

1. Decreasing welding speed and placing the hard material (copper) on the advancing side of the tool, while using a 2 mm offset of the tool lead to lower welding forces on the tool. On the other hand, placing copper at the retreating side leads to higher forces even with the presence of an offset.
2. The lack of tool offset during welding aluminum to copper appears to be the reason for presence of voids in the weld nugget. Furthermore, placing the softer material at the advancing side of the pin tool during friction stir welding of dissimilar materials produces defects.
3. Large voids were produced when the traditional method of inserting the pin tool in the weld line of butted plates is used.
4. It is possible to friction stir weld copper to Al6061-T6 and obtains sound weldment with relatively low welding force when copper is placed at the

advancing side of the tool and when using tool offset of 2 mm towards the retreating side.

5. The elements and phases present in the aluminum to copper weld nugget included single phases of Al_2Cu, AlCu, Al_4Cu_9, and Solid Solution Al (Cu) in addition to a two phase (Al+ Al_2Cu).
6. In general, the hardness values of the aluminum to copper weld nugget were greater than those of the two base metals. Furthermore, hardness is higher at the copper side interface (with the nugget) compared to the aluminum side interface (with the nugget) and to the weld nugget zone.
7. The coupled Eulerian Lagrangian (CEL) model was able to simulate the FSW process of similar commercial pure copper butt joint and predict the temperature in the weld bead at an accuracy level of 10% for the axial forces and 3.7% for temperature.

6.2 Recommendations

This research work represents the basement to break through the friction stir welding of dissimilar metals and alloys and from the results we recommend the following:

1. The work related to the similar friction stir welding of commercial pure copper can be expanded to involve other welding parameters.
2. Study the effects of dwell time and plunging rate on weld quality.
3. The investigation of the process parameters effects on dissimilar FSW welding of aluminum with copper opens the door toward other dissimilar metals and alloys i.e. steel with Copper-Nickel as in the tube-tube sheet heat exchangers or aluminum with steel as in the automobile industry as well as the dissimilar aluminum alloys on the aircraft field.

APPENDICES

Appendix A: EDS Profile and Possible Al/Cu Phases, Table 3.1

Condition No. 3

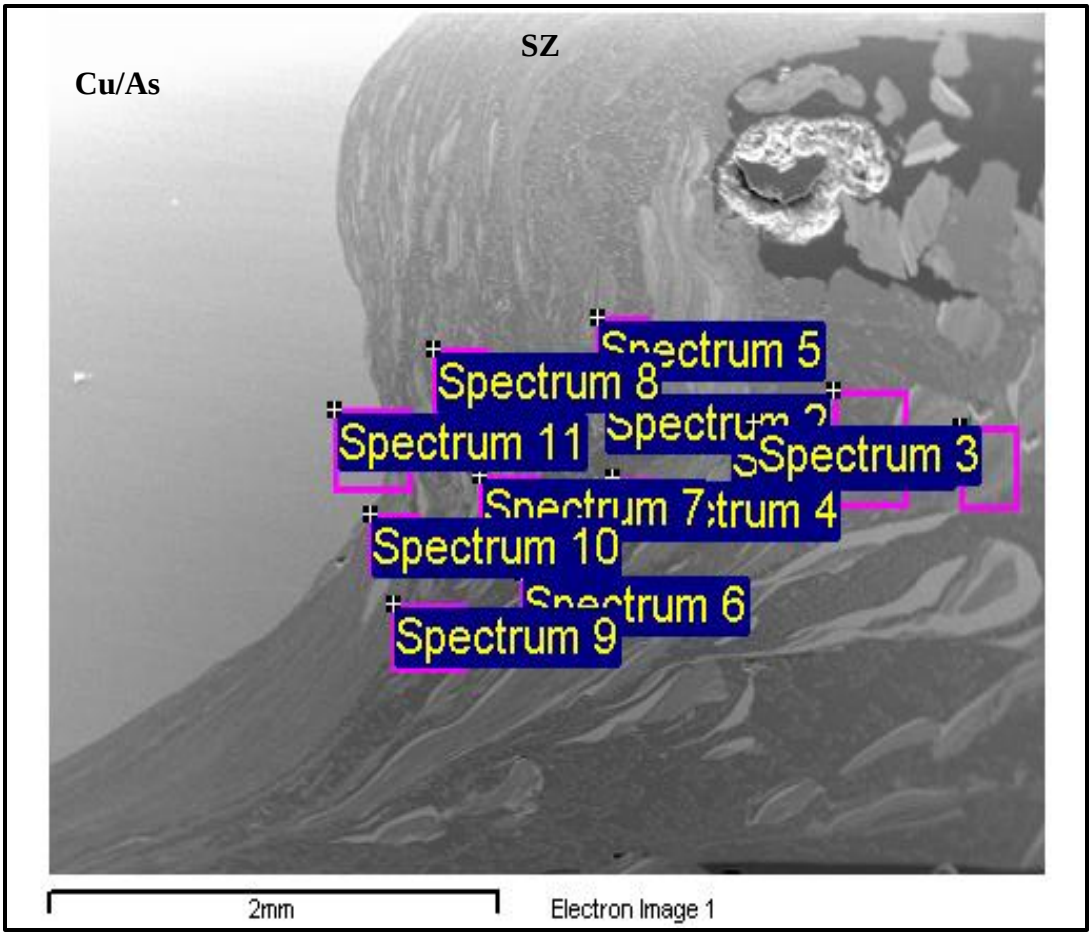

Fig. A.1: EDS Locations toward Copper Side

Table A.1: Fig. A.1 Spectrum analysis toward Cu side

Spectrum	Al Wt.%	Cu Wt.%	Possible Phases
1	69.55	30.45	Al_2Cu
2	76.17	23.14	Al_2Cu
3	92.87	6.36	Solid Solution Al (Cu)
4	86.74	12.46	Al+ Al_2Cu
5	84.31	14.95	Al+ Al_2Cu
6	75.23	24.04	Al_2Cu
7	67.1	32.05	Al_2Cu
8	72.05	27.23	Al_2Cu
9	82.33	16.89	Al+ Al_2Cu
10	52.66	46.75	AlCu
11	29.78	70.22	Al_4Cu_9

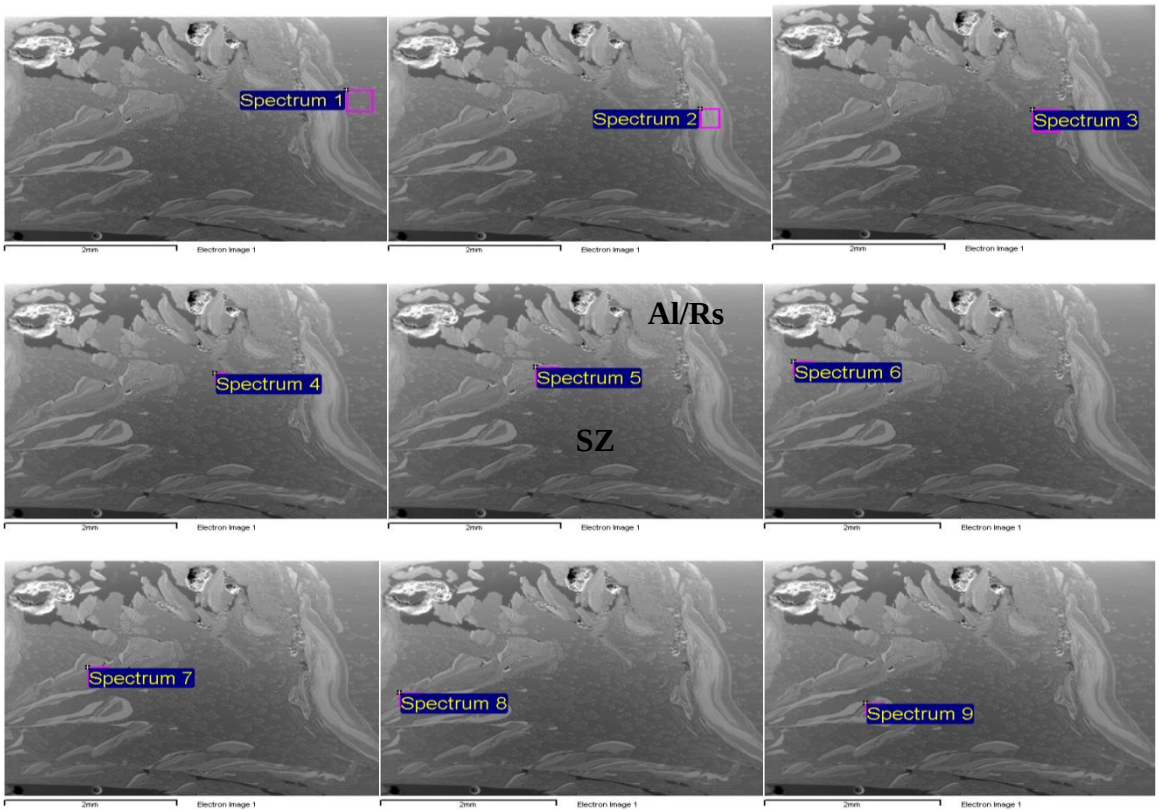

Fig. A.2: EDS Locations toward Al6061-T6 Side

Table A.2: Fig. A.2 Spectrum analysis toward Al6061-T6 side

Spectrum	Al Wt.%	Cu Wt.%	Possible Phase
1	94.44	4.75	Solid Solution Al (Cu)
2	19.05	80.95	Al_4Cu_9
3	90.89	6.78	Solid Solution Al (Cu)
4	93.54	5.65	Solid Solution Al (Cu)
5	64.32	34.96	Al_2Cu
6	93.72	5.35	Solid Solution Al (Cu)
7	71.71	27.62	Al_2Cu
8	61.30	37.85	Al_2Cu
9	55.38	44.62	AlCu

Appendix B: Inference Calculations for Copper Tensile Strength Data

Table B.1: Hypothesis & Interference analysis of similar Cu tensile strength joints, 95% confidence interval

Vw=100		Vw=125		Vw=150		
Max.Tensile Mpa	El.%	Max.Tensile Mpa	El.%	Max.Tensile Mpa	El.%	
217.3	47.42	214.71	47.74	209.98	42.2	
215.68	48.74	219.02	49.56	217.96	51.94	
213.6	49.47	218.41	46.58	213.36	52.77	
X_1	X2	X_3	S_1	S_2	S_3	
215.527	217.380	213.767	2.623	3.298	5.665	
S_1^2	S_2^2	S_3^2	X_2-X_1	X_2-X_3	V_{2-1}	V_{2-3}
6.880	10.879	32.088	1.853	3.613	3.807	3.216
< μ2-μ1	>μ2-μ1	< μ2-μ3	> μ2-μ1			
-3.334	7.041	-5.292	12.518			

Appendix C: Commercial Pure Copper Properties

Table C.1: Copper Mechanical and Thermal Properties variation with temperature [43]

Temp. (°C)	Modulus of Elasticity, E (GPa)	v	Thermal Expansion, α, (1/K)	Temp. (°C)	Thermal Conductivity (m/W.K)	Temp. (°C)	Temp. (°C)	C_p (J/Kg.K)
294	117.2	0.3	16.70	293	401	273	100	255
366	114.457	0.3	17.30	350	398	300	200	494
422	112.388	0.3	17.60	400	394	350	273.5	379.7
477	110.32	0.3	18.30	500	392	400	280	381.1
533	107.562	0.3	18.90	600	388	500	293	386
589	104.11	0.3	19.60	700	383	600	298.15	384.6
644	99.977	0.3	20.40	800	377	700	300	384.9
-	-	-	22.40	1000	371	800	558.273	411.003
-	-	-	24.80	1100	350	900	607.304	416.03
-	-	-	-	1200	364	1000	662.508	420.39

Appendix D: Commercial Pure Copper Butt joints Hardness Results

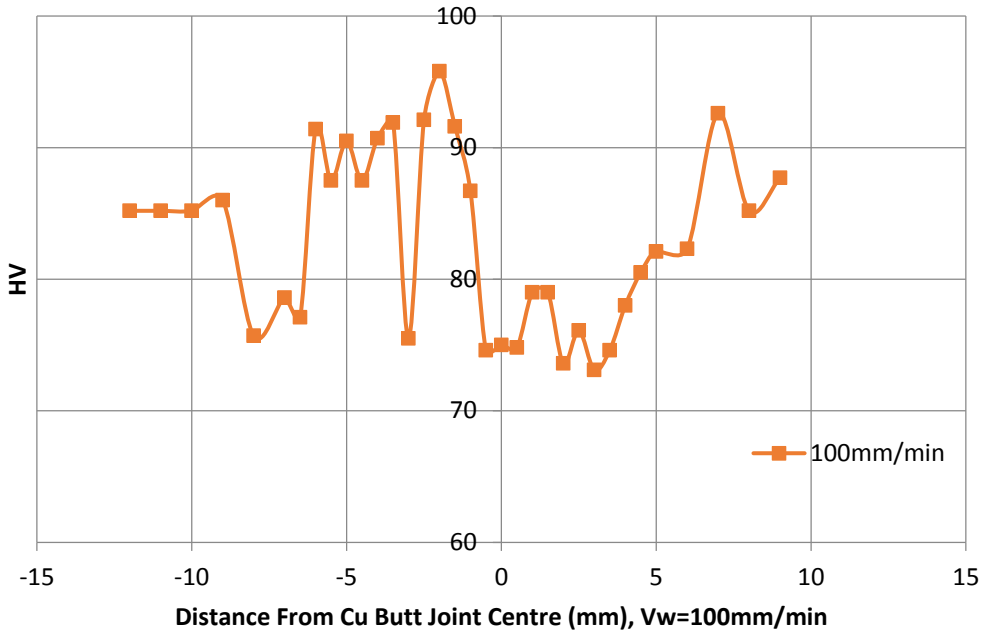

Fig. D.1: Vickers Micro Hardness distributions at 100mm/min Welding Speed and 900rpm rotational speed

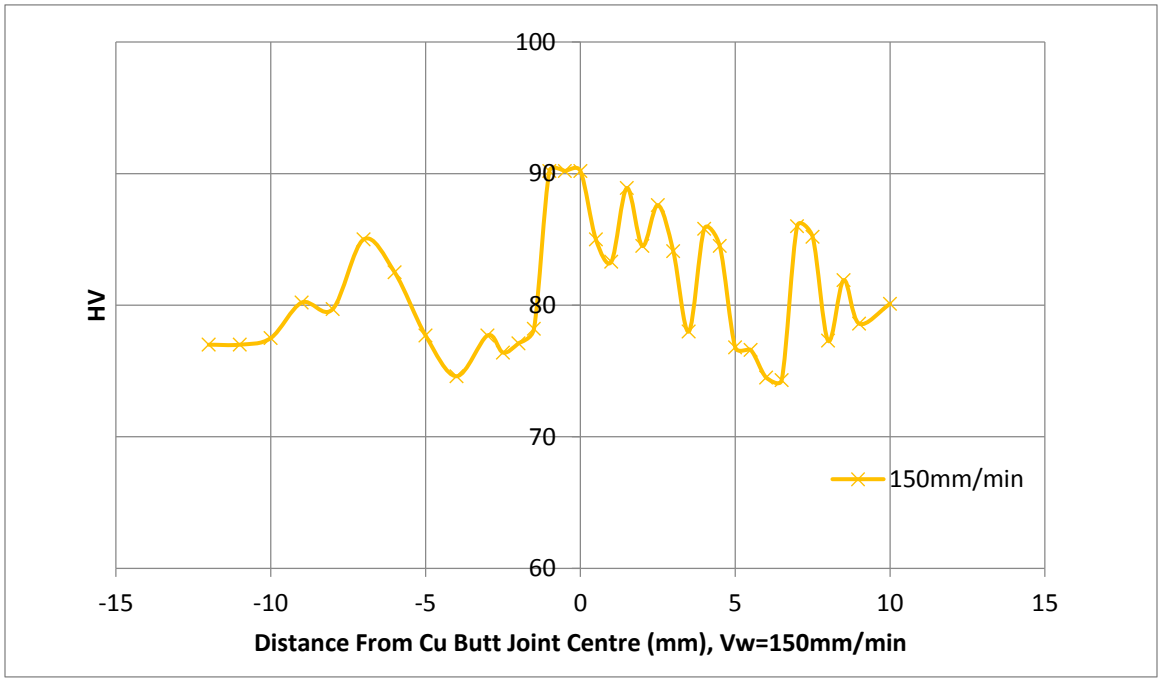

Fig. D.2: Vickers Micro Hardness distributions at 150mm/min Welding Speed and 900rpm rotational speed

Appendix E: CEL Model Input File

** Job name: Job-1-Al-Cu-900-40-2mm Model name: ASME model-Offset-2mm

** Generated by: Abaqus/CAE 6.13-1

*Preprint, echo=NO, model=NO, history=NO, contact=NO

** PARTS

*Part, name="temp-Threaded tool-38-new"

*Element, type=C3D4T

*Elset, elset=Initially Invalid 6061, 8075

*Nset, nset=_PickedSet11, internal, generate 1, 10991, 1

*Elset, elset=_PickedSet11, internal, generate1, 57568, 1

** Section: tool

*Solid Section, elset=_PickedSet11, material=Material-Too,

*End Part

*Elset, elset=_Bootom-Al_S2, internal, instance=workpiece-1, generate

274068, 280852, 1

*Elset, elset=_Bootom-Al_S6, internal, instance=workpiece-1, generate

66001, 125991, 10

*Surface, type=ELEMENT, name=Bootom-Al

_Bootom-Al_S2, S2

_Bootom-Al_S6, S6

*Elset, elset=_Bottom-Cu_S2, internal, instance=workpiece-1, generate

199471, 206217, 1

*Elset, elset=_Bottom-Cu_S4, internal, instance=workpiece-1, generate

6010, 66000, 10

*Surface, type=ELEMENT, name=Bottom-Cu

_Bottom-Cu_S2, S2

_Bottom-Cu_S4, S4

*Elset, elset=_Top-Al_S1, internal, instance=workpiece-1, generate

213003, 219787, 1

*Elset, elset=_Top-Al_S4, internal, instance=workpiece-1, generate

66010, 126000, 10

*Surface, type=ELEMENT, name=Top-Al

_Top-Al_S1, S1

_Top-Al_S4, S4

*Elset, elset=_Top-Cu_S1, internal, instance=workpiece-1, generate

138748, 145494, 1

*Elset, elset=_Top-Cu_S6, internal, instance=workpiece-1, generate

6001, 65991, 10

*Surface, type=ELEMENT, name=Top-Cu

_Top-Cu_S1, S1

_Top-Cu_S6, S6

*Nset, nset="_T-tool datum", internal

_PickedSet18,

_PickedSet17,

*Transform, nset="_T-tool datum"

0.99862953619093, 0.0523358158245099, 0.000108761531622454, -0.0523358215911015, 0.998629540515884, 5.08666861727711e-05

** Constraint: Constraint-RP

*Rigid Body, ref node=_PickedSet15, elset=_PickedSet16

*End Assembly

*Amplitude, name=Amp-exit

0., 0, 0.001, 1.

*Amplitude, name=Amp-plunging

0., 0, 0.0117, 1.

** MATERIALS

*Material, name=Material-Al-6061-T6

*Conductivity

140000., 298.

168000., 373.

183000., 477.44

208000., 588.56

222000., 699.67

220000., 755.22

*Density 2700.,

*Elastic

6.694e+10, 0.33, 298.

6.321e+10, 0.334, 373.

5.68e+10, 0.336, 477.44

4.717e+10, 0.36, 588.56

2.877e+10, 0.41, 699.67

2.02e+10, 0.42, 755.22

*Expansion, zero=298.

2.34e-05,298.

2.46e-05,373.

2.56e-05,423.

2.66e-05,473.

2.75e-05,523.

2.85e-05,573.

3.07e-05,623.

*Inelastic Heat Fraction 0.9,

*Plastic, hardening=JOHNSON COOK

3.24e+08, 1.14e+08, 0.42, 1.34, 855, 298.

*Rate Dependent, type=JOHNSON COOK 0.002,1000.

*Specific Heat

870., 298.

920., 373.

960., 477.44

1040., 588.56

1180., 699.67

1280., 755.22

*Material, name=Material-Cu

*Conductivity

401000., 273.

398000., 300.

394000., 350.

392000., 400.

388000., 500.

383000., 600.

377000., 700.

371000., 800.

364000., 900.

357000.,1000.

350000.,1100.

*Density 8940.,

*Elastic

1.172e+11, 0.33, 294.

1.14457e+11, 0.333, 366.

1.12388e+11, 0.335, 422.

1.1032e+11, 0.34, 477.

1.07562e+11, 0.345, 533.

1.0411e+11, 0.35, 589.

9.9977e+10, 0.36, 644.

*Expansion, zero=298.

1.67e-05, 293.

1.73e-05, 350.

1.76e-05, 400.

1.83e-05, 500.

1.89e-05, 600.

1.96e-05, 700.

2.04e-05, 800.

2.24e-05,1000.

2.48e-05,1200.

*Inelastic Heat Fraction 0.9,

*Plastic, hardening=JOHNSON COOK

9e+07, 2.92e+08, 0.31, 1.09, 1356., 298.

*Rate Dependent, type=JOHNSON COOK 0.025,1000.

*Specific Heat

255., 100.

494., 200.

379.7, 273.5

381.1, 280.

386., 293.

384.6, 298.15

384.9, 300.

411.003, 558.273

416.03, 607.304

420.39, 662.508

424.718, 709.513

427.656, 754.515

431.984, 801.52

434.851, 828.073

437.081, 868.999

440.671, 903.729

444.975, 944.584

448.62, 993.662

452.21, 1028.39

455.823, 1069.27

458.062, 1112.25

461.643, 1144.93

464.526, 1175.58

468.139, 1216.46

471.038, 1251.21

472.546, 1283.96

476.191, 1333.04

*Material, name=Material-Tool

*Conductivity29.,

*Density 7.8e+06,

*Elastic2e+11, 0.3

*Specific Heat 460.,

** INTERACTION PROPERTIES

*Surface Interaction, name=IntProp-contact

*Friction 0.5,

*Surface Behavior, pressure-overclosure=HARD

*Gap Heat Generation 1., 0.5

** PHYSICAL CONSTANTS

*Physical Constants, absolute zero=0., stefan boltzmann=5.67e-05

** BOUNDARY CONDITIONS

** Name: BC-3 workpiece Type: Velocity/Angular velocity

*Boundary, type=VELOCITY _PickedSet19, 3, 3

** Name: BC-4 workpiece Type: Velocity/Angular velocity

*Boundary, type=VELOCITY_PickedSet30, 1, 1

** Name: BC-5 bottom Type: Velocity/Angular velocity

*Boundary, type=VELOCITY_PickedSet31, 2, 2

** PREDEFINED FIELDS

** Name: Eulerain Temp Type: Temperature

*Initial Conditions, type=TEMPERATURE

"Eulerain Plate", 298.

** Name: Predefined Field-5 Type: Material assignment

*Initial Conditions, type=VOLUME FRACTION

Al-Plate, workpiece-1.Al, 1.

Cu-Plate, workpiece-1.copper, 1.

** Name: Tool Temp Type: Temperature

*Initial Conditions, type=TEMPERATURE

"temp-Threaded tool-38-new-1".InitiallyInvalid, 298.

** Name: Void Temp Type: Temperature

*Initial Conditions, type=TEMPERATURE

void, 298.

** INTERACTIONS

** Interaction: contact

*Contact, op=NEW

*Contact Inclusions, ALL EXTERIOR

*Contact Property Assignment, IntProp-contact

** STEP: Step-plunging

*Step, name=Step-plunging, nlgeom=YES

*Dynamic Temperature-displacement, Explicit

, 0.0114

*Bulk Viscosity 0.06, 1.2

** BOUNDARY CONDITIONS

** Name: BC-2 tool displacement Type: Displacement/Rotation

*Boundary, amplitude=Amp-plunging

_PickedSet18, 1, 1

_PickedSet18, 2, 2, -0.0038

_PickedSet18, 3, 3

_PickedSet18, 4, 4

_PickedSet18, 6, 6

** Name: BC-tool velocity Type: Velocity/Angular velocity

*Boundary, type=VELOCITY

_PickedSet17, 5, 5, -94247.8

** INTERACTIONS

** Interaction: Conduction-Back-Al

*Sfilm

Bootom-Al, F, 298., 1e+06

** Interaction: Convection Top-Al

*Sfilm

Top-Al, F, 298., 25000.

** Interaction: Radiation-Al

*Sradiate

Top-Al, R, 298., 0.1

** Interaction: conduction bot

*Sfilm

Bottom-Cu, F, 298., 2e+06

** Interaction: convective top-Cu

*Sfilm

Top-Cu, F, 298., 25000.

** Interaction: radiation top

*Sradiate

Top-Cu, R, 298., 0.64

** OUTPUT REQUESTS

*Restart, write, number interval=1, time marks=NO

** FIELD OUTPUT: F-Output-1

*Output, field, time interval=5e-05

*Node Output

A, NT, RF, RFL, U, V

*Element Output, directions=YES

EVF, HFL, LE, PE, PEEQ, PEEQVAVG, PEVAVG, S, SVAVG, TEMP

*Contact Output

CSTRESS, FSLIPR

** HISTORY OUTPUT: H-Output-1

*Output, history, variable=PRESELECT, time interval=0.001

*End Step

** STEP: Step-dwell

*Step, name=Step-dwell, nlgeom=YES

*Dynamic Temperature-displacement, Explicit , 0.002

*Bulk Viscosity 0.06, 1.2

** BOUNDARY CONDITIONS

** Name: BC-2 tool displacement Type: Displacement/Rotation

*Boundary, amplitude=Amp-plunging_PickedSet18, 2, 2

** OUTPUT REQUESTS

*Restart, write, number interval=1, time marks=NO

** FIELD OUTPUT: F-Output-1

*Output, field, time interval=5e-05

*Node Output

A, NT, RF, RFL, U, V

*Element Output, directions=YES

EVF, HFL, LE, PE, PEEQ, PEEQVAVG, PEVAVG, S, SVAVG, TEMP

*Contact Output

CSTRESS, FSLIPR

** HISTORY OUTPUT: H-Output-1

*Output, history, variable=PRESELECT, time interval=0.001

*End Step

** STEP: Step-welding

*Step, name=Step-welding, nlgeom=YES

*Dynamic Temperature-displacement, Explicit , 0.02

*Bulk Viscosity0.06, 1.2

** BOUNDARY CONDITIONS

** Name: BC-2 tool displacement Type: Displacement/Rotation

*Boundary, op=NEW, amplitude=Amp-plunging

_PickedSet18, 3, 3

_PickedSet18, 4, 4

_PickedSet18, 6, 6

** Name: BC-3 workpiece Type: Velocity/Angular velocity

*Boundary, op=NEW, type=VELOCITY

_PickedSet19, 3, 3

** Name: BC-4 workpiece Type: Velocity/Angular velocity

*Boundary, op=NEW, type=VELOCITY

_PickedSet30, 1, 1

** Name: BC-5 bottom Type: Velocity/Angular velocity

*Boundary, op=NEW, type=VELOCITY

_PickedSet31, 2, 2

** Name: BC-tool velocity Type: Velocity/Angular velocity

*Boundary, op=NEW, type=VELOCITY

_PickedSet17, 1, 1, 0.6657

_PickedSet17, 2, 2, -0.03489

_PickedSet17, 5, 5, -94247.8

** OUTPUT REQUESTS

*Restart, write, number interval=1, time marks=NO

** FIELD OUTPUT: F-Output-1

*Output, field, time interval=5e-05

*Node Output

A, NT, RF, RFL, U, V

*Element Output, directions=YES

EVF, HFL, LE, PE, PEEQ, PEEQVAVG, PEVAVG, S, SVAVG, TEMP

*Contact Output

CSTRESS, FSLIPR

** HISTORY OUTPUT: H-Output-1

*Output, history, variable=PRESELECT, time interval=0.001

*End Step

** STEP: Step-exit

*Step, name=Step-exit, nlgeom=YES

*Dynamic Temperature-displacement, Explicit

, 0.001

*Bulk Viscosity

0.06, 1.2

** BOUNDARY CONDITIONS

** Name: BC-2 tool displacement Type: Displacement/Rotation

*Boundary, op=NEW, amplitude=Amp-exit

_PickedSet18, 1, 1

_PickedSet18, 2, 2, 0.004

_PickedSet18, 3, 3

_PickedSet18, 4, 4

_PickedSet18, 6, 6

** Name: BC-3 workpiece Type: Velocity/Angular velocity

*Boundary, op=NEW, type=VELOCITY

_PickedSet19, 3, 3

** Name: BC-4 workpiece Type: Velocity/Angular velocity

*Boundary, op=NEW, type=VELOCITY

_PickedSet30, 1, 1

** Name: BC-5 bottom Type: Velocity/Angular velocity

*Boundary, op=NEW, type=VELOCITY

_PickedSet31, 2, 2

** Name: BC-tool velocity Type: Velocity/Angular velocity

*Boundary, op=NEW, type=VELOCITY

_PickedSet17, 5, 5, -94247.8

** OUTPUT REQUESTS

*Restart, write, number interval=1, time marks=NO

** FIELD OUTPUT: F-Output-1

*Output, field, time interval=5e-05

*Node Output

A, NT, RF, RFL, U, V

*Element Output, directions=YES

EVF, HFL, LE, PE, PEEQ, PEEQVAVG, PEVAVG, S, SVAVG, TEMP

*Contact Output

CSTRESS, FSLIPR

** HISTORY OUTPUT: H-Output-1

*Output, history, variable=PRESELECT, time interval=0.001

*End Step*Part, name=workpiece

NOMENCLATURE

A	Material constant (MPa)
As	Advancing Side
B	Material constant (MPa)
BM	Base Metal
C_p	specific heat (J/kg·K)
c	strain rate sensitivity
E	Modulus of Elasticity (GPa)
El %.	Elongation Percent
Fn	Normal force on the tool (KN)
HAZ	Heat Affected Zone
HV	Vickers hardness
K	Thermal conductivity (W/m•K)
m	Thermal softening effect
Mpa	Mega Pascal
n	Parameters takes into account the effect of strain hardening
N	Tool rotational speed (rpm)
q	Heat Flux (W/m^2)
Qp	Heat generation from the pin (W)
Qs	Heat generation from the shoulder (W)
Qt	Total heat generation from FSW tool (W)
Rp	Pin radius (mm)
Rs	Reterating side
Rsh	Shoulder radius (mm)
S	Standard Diviation
SZ	Stir Zone
T	Temperature (K)
TMAZ	Thermo Mechanical Affected Zone
Tmelt	Material solidus temperature (K)

Tref	Temperature where A, B and n are evaluated i.e. 293K
u	mass flow rate (kg/s)
v	Poison's Ratio
V	Degrees of freedom
Vweld	Welding Speed (mm/sec)
Wt %.	Weight Percent
X	Mean of independent random sample

Greek letters

α	Thermal Expansion (1/K)
$\varepsilon_{pl}^{\overline{n}}$	Effective plastic strain
$\overline{\dot{\varepsilon}}_{\text{pl}}$	Effective plastic strain rate
$\dot{\varepsilon}o$	normalizing strain rate (typically 1.0s)
μ	Coefficient of friction, Dynamic Viscosity (Pa.Sec), Confidence Interval
ν	kinematic viscosity (m^2/s)
ρ	density (kg/m^3)
σo	Flow stress (Pa)

REFERENCES

[1] R. S. Mishra and Z. Y. Ma, "Friction stir welding and processing," *Mater. Sci. Eng. R Reports*, vol. 50, no. 1–2, pp. 1–78, Aug. 2005.

[2] V. Soundararajan, "Thermo-Mechanical and Microstructural Issues in Joining Similar and Dissimilar Metals by Friction Stir Welding, Phd Dissertation," Southern Methodist University, 2006.

[3] M. Nicholas, "Material aspects of ceramic-ceramic and ceramic-metal bonding," *Adv. Join. Technol.*, no. Springer, pp. 160–171, 1990.

[4] C. W. Tan, Z. G. Jiang, L. Q. Li, Y. B. Chen, and X. Y. Chen, "Microstructural evolution and mechanical properties of dissimilar Al–Cu joints produced by friction stir welding," *Mater. Des.*, vol. 51, pp. 466–473, Oct. 2013.

[5] A. S. and N. Merah, "The National Plan for Science, Technology and Innovation (NPST) Project No-08-ADV66-04."

[6] a. Scialpi, L. a. C. De Filippis, and P. Cavaliere, "Influence of shoulder geometry on microstructure and mechanical properties of friction stir welded 6082 aluminium alloy," *Mater. Des.*, vol. 28, no. 4, pp. 1124–1129, Jan. 2007.

[7] S. Malarvizhi and V. Balasubramanian, "Influences of tool shoulder diameter to plate thickness ratio (D/T) on stir zone formation and tensile properties of friction stir welded dissimilar joints of AA6061 aluminum–AZ31B magnesium alloys," *Mater. Des.*, vol. 40, pp. 453–460, Sep. 2012.

[8] K. Elangovan and V. Balasubramanian, "Influences of pin profile and rotational speed of the tool on the formation of friction stir processing zone in AA2219 aluminium alloy," *Mater. Sci. Eng. A*, vol. 459, no. 1–2, pp. 7–18, Jun. 2007.

[9] O. Lorrain, V. Favier, H. Zahrouni, and D. Lawrjaniec, "Understanding the material flow path of friction stir welding process using unthreaded tools," *J. Mater. Process. Technol.*, vol. 210, no. 4, pp. 603–609, Mar. 2010.

[10] K. J. Colligan and R. S. Mishra, "A conceptual model for the process variables related to heat generation in friction stir welding of aluminum," *Scr. Mater.*, vol. 58, no. 5, pp. 327–331, 2008.

[11] P. Chaitanya Sharma, Dheerendra Kumar Dwivedi, "Effect of welding parameters on microstructure and mechanical properties of friction stir welded joints of AA7039 aluminum alloy," *Mater. Des.*, vol. 36, p. 379, 2010.

[12] I. Dinaharan, K. Kalaiselvan, S. J. Vijay, and P. Raja, “Effect of material location and tool rotational speed on microstructure and tensile strength of dissimilar friction stir welded aluminum alloys,” *Arch. Civ. Mech. Eng.*, vol. 12, no. 4, pp. 446–454, Dec. 2012.

[13] M. Koilraj, V. Sundareswaran, S. Vijayan, and S. R. Koteswara Rao, “Friction stir welding of dissimilar aluminum alloys AA2219 to AA5083 – Optimization of process parameters using Taguchi technique,” *Mater. Des.*, vol. 42, pp. 1–7, Dec. 2012.

[14] H. Lombard, D. G. Hattingh, a. Steuwer, and M. N. James, “Optimising FSW process parameters to minimise defects and maximise fatigue life in 5083-H321 aluminium alloy,” *Eng. Fract. Mech.*, vol. 75, no. 3–4, pp. 341–354, Feb. 2008.

[15] L. E. Murr, “A Review of FSW Research on Dissimilar Metal and Alloy Systems,” *J. Mater. Eng. Perform.*, vol. 19, no. 8, pp. 1071–1089, Feb. 2010.

[16] T. Sakthivel and J. Mukhopadhyay, “Microstructure and mechanical properties of friction stir welded copper,” *J. Mater. Sci.*, vol. 42, no. 19, pp. 8126–8129, Jun. 2007.

[17] Y. F. Sun and H. Fujii, “Investigation of the welding parameter dependent microstructure and mechanical properties of friction stir welded pure copper,” *Mater. Sci. Eng. A*, vol. 527, no. 26, pp. 6879–6886, Oct. 2010.

[18] K.-T. Huang, T.-S. Lui, and L.-H. Chen, “Effect of Microstructural Feature on the Deterioration of Tensile Properties and Vibration Fracture Resistance of FSW 5052-H34 Alloy,” *Mater. Trans.*, vol. 45, no. 11, pp. 3216–3222, 2004.

[19] a. Heidarzadeh, T. Saeid, H. Khodaverdizadeh, a. Mahmoudi, and E. Nazari, “Establishing a Mathematical Model to Predict the Tensile Strength of Friction Stir Welded Pure Copper Joints,” *Metall. Mater. Trans. B*, vol. 44, no. 1, pp. 175–183, Oct. 2012.

[20] H. Pashazadeh, J. Teimournezhad, and A. Masoumi, “Numerical investigation on the mechanical, thermal, metallurgical and material flow characteristics in friction stir welding of copper sheets with experimental verification,” *Mater. Des.*, vol. 55, pp. 619–632, Mar. 2014.

[21] M. Jabbari, “Elucidating of rotation speed in friction stir welding of pure copper: Thermal modeling,” *Comput. Mater. Sci.*, vol. 81, pp. 296–302, Jan. 2014.

[22] X. Li, D. Zhang, C. Qiu, and W. Zhang, “Microstructure and mechanical properties of dissimilar pure copper/1350 aluminum alloy butt joints by friction

stir welding," *Trans. Nonferrous Met. Soc. China*, vol. 22, no. 6, pp. 1298–1306, Jun. 2012.

[23] I. Galvão, D. Verdera, D. Gesto, a. Loureiro, and D. M. Rodrigues, "Influence of aluminium alloy type on dissimilar friction stir lap welding of aluminium to copper," *J. Mater. Process. Technol.*, vol. 213, no. 11, pp. 1920–1928, Nov. 2013.

[24] J. Ouyang, E. Yarrapareddy, and R. Kovacevic, "Microstructural evolution in the friction stir welded 6061 aluminum alloy (T6-temper condition) to copper," *J. Mater. Process. Technol.*, vol. 172, no. 1, pp. 110–122, Feb. 2006.

[25] I. Galvão, R. M. Leal, D. M. Rodrigues, and A. Loureiro, "Journal of Materials Processing Technology Influence of tool shoulder geometry on properties of friction stir welds in thin copper sheets," vol. 213, pp. 129–135, 2013.

[26] P. Xue, D. R. Ni, D. Wang, B. L. Xiao, and Z. Y. Ma, "Effect of friction stir welding parameters on the microstructure and mechanical properties of the dissimilar Al–Cu joints," *Mater. Sci. Eng. A*, vol. 528, no. 13–14, pp. 4683–4689, May 2011.

[27] I. Galvão, A. Loureiro, D. Verdera, D. Gesto, and D. M. Rodrigues, "Influence of Tool Offsetting on the Structure and Morphology of Dissimilar Aluminum to Copper Friction-Stir Welds," *Metall. Mater. Trans. A*, vol. 43, no. 13, pp. 5096–5105, Aug. 2012.

[28] I. Galvão, R. M. Leal, a. Loureiro, and D. M. Rodrigues, "Material flow in heterogeneous friction stir welding of aluminium and copper thin sheets," *Sci. Technol. Weld. Join.*, vol. 15, no. 8, pp. 654–660, Nov. 2010.

[29] E. T. Akinlabi and S. A. Akinlabi, "Effect of Heat Input on the Properties of Dissimilar Friction Stir Welds of Aluminium and Copper," *Am. J. Mater. Sci.*, vol. 2, no. 5, pp. 147–152, Dec. 2012.

[30] M. Song and R. Kovacevic, "Thermal modeling of friction stir welding in a moving coordinate system and its validation," *Int. J. Mach. Tools Manuf.*, vol. 43, no. 6, pp. 605–615, May 2003.

[31] H.-H. Cho, S.-T. Hong, J.-H. Roh, H.-S. Choi, S. H. Kang, R. J. Steel, and H. N. Han, "Three-dimensional numerical and experimental investigation on friction stir welding processes of ferritic stainless steel," *Acta Mater.*, vol. 61, no. 7, pp. 2649–2661, Apr. 2013.

[32] P. a. Colegrove and H. R. Shercliff, “3-Dimensional CFD modelling of flow round a threaded friction stir welding tool profile,” *J. Mater. Process. Technol.*, vol. 169, no. 2, pp. 320–327, Nov. 2005.

[33] R. S.R., H. S. Bang, W. S. Chang, H. J. Kim, H. S. Bang, C. I. Oh, and J. S. Chu, “Numerical determination of residual stress in friction stir weld using 3D-analytical model of stir zone,” *J. Mater. Process. Technol.*, vol. 187–188, pp. 224–226, Jun. 2007.

[34] G. Buffa, J. Hua, R. Shivpuri, and L. Fratini, “A continuum based fem model for friction stir welding—model development,” *Mater. Sci. Eng. A*, vol. 419, no. 1–2, pp. 389–396, Mar. 2006.

[35] N. S. binti Sataruddin, M. Awang, and K. Z. K. Shaari, “Material flow study during friction stir welding process using computational fluid dynamics simulation,” *2011 Natl. Postgrad. Conf.*, pp. 1–4, Sep. 2011.

[36] Fadi Abdel Kareem Al-Badour, “Friction Stir Welding Of Tube-Tube Sheet Joints,” King Fahd University of Petroleum and Minerals, 2012.

[37] American society for testing and materials (ASTM). In: Standard test methods for tension testing of metallic materials, ASTM E8M – 09, vol. 03.01. West Conshohocken (PA): Annual book of ASTM standards;. .

[38] “Abaqus®.”

[39] G. R. J. William H.Cook, “A constitutive Model and Data for Materials Subjected to Large Strains, High Starin Rates and High Temperatures,” in *Proceedings 7th International Symp. on Ballistics*, 1983.

[40] M. KUTZ, Ed., Mechanical Engineers Handbook, Second Edi. JOHN WILEY & SONS9 INC., 1998.

[41] F. Al-Badour, N. Merah, A. Shuaib, and A. Bazoune, “Coupled Eulerian Lagrangian finite element modeling of friction stir welding processes,” *J. Mater. Process. Technol.*, vol. 213, no. 8, pp. 1433–1439, Aug. 2013.

[42] A. H. ASM International, *Alloy Phase Diagrams*. 1992.

[43] A. H. ASM International, “Copper and Copper Alloys,” 2002.

Vitae

Name : Gihad Mohamed Karrar Babekr

Nationality : Sudanese

Date of Birth : 25th February 1988

Email : gehad0451@hotmail.com;

Address : Khartoum, Sudan

Academic Background :

MSc. (Mechanical Engineering)

January 2015

King Fahd University of Petroleum and Minerals

Dhahran, Saudi Arabia.

BSc. (Mechanical Engineering)

August 2009

University of Khartoum

Khartoum, Sudan.

Publications :

1. Friction stir welding of commercially pure copper plates, Gihad Karrar, Abdelrahman Shuaib, Fadi Albador, Nesar Merah, A. M Mahjoub, the ASME 2014 International Mechanical Engineering Congress & Exposition, Montreal, Canada, IMECE2014-38378, (Published).
2. Experimental Study and Numerical modeling of Friction Stir Spot Welding of Copper Lap Joint, Ahmed Mahgoub, Abdelaziz Bazoune, Fadi Al-Badour, Abdelrahman Shuaib, Gihad Karrar, the ASME 2014 International Mechanical Engineering Congress & Exposition, Montreal, Canada, IMECE2014- 38033, (Published).
3. Joining Aluminum A6061-T6 and Copper Plates using Friction Stir Welding, Gihad Karrar, A.N. Shuaib, F. Al-Badour, N. Merah , and A. Bazoune, Journal of Manufacturing Science and Engineering, MANU-14-1707 (Submitted and Under Review).
4. Friction stir welding of commercially pure copper plates, Gihad Karrar, Abdelrahman Shuaib, Fadi Albador, Nesar Merah, and A. Bazoune, Journal of Manufacturing Science and Engineering, MANU-14-1710, (Submitted and Under Review).

References :

Dr. Abdelrahman Nasr Shuaib (e-mail: arshuaib@kfupm.edu.sa)

Dr. Nesar Ammar Salah Merah (e-mail: nesar@kfupm.edu.sa)

Dr. Abdelaziz Bazoune (e-mail: abazoune@kfupm.edu.sa)

Dr. Omer Alfarog Albadawy (e-mail: oeelbadawi@uofk.edu)